

Electronic Supplementary Information for Mono- and Tri- β -Substituted Unsymmetrical Metalloporphyrins: Synthesis, Structural, Spectral and Electrochemical Properties

Kamal Prakash, Ravi Kumar and Muniappan Sankar*

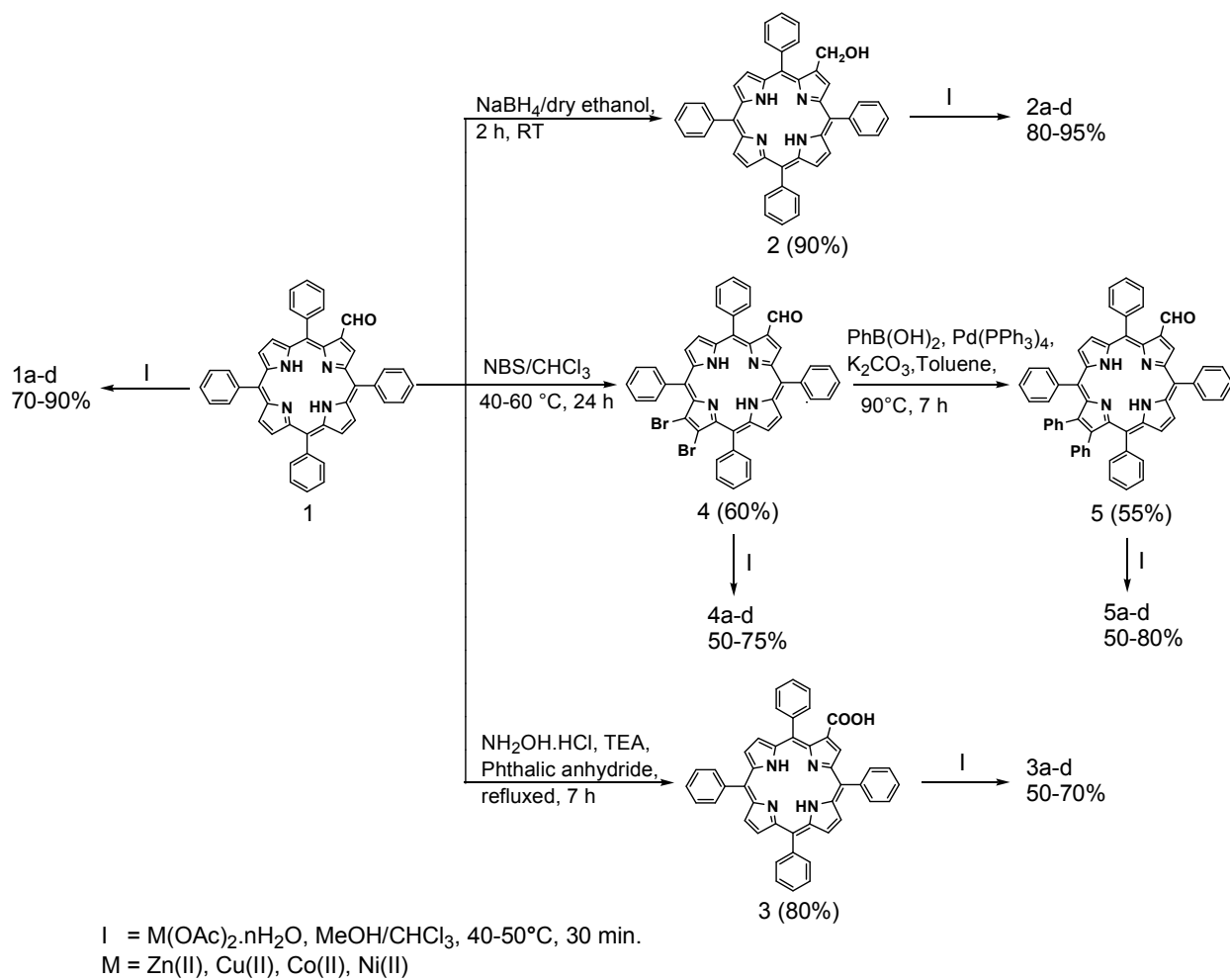
^[a]Department of Chemistry, Indian Institute of Technology Roorkee, Roorkee – 247667, India

Table of contents (TOC)

	Page No
Scheme S1. Synthetic scheme for MTPP(X)Y ₂ .	4
Figure S1. B3LYP/ 6-311g(d,p) optimised geometries showing top as well as side views of H ₂ TPP(CHO) (a and d), H ₂ TPP(CH ₂ OH) (b and e) and H ₂ TPP(COOH) (c and f), respectively. In side view, the β -substituents and <i>meso</i> -phenyl groups are not shown for clarity. The displacement of porphyrin-core atoms in Å from the mean plane are shown in figures g , h and i for H ₂ TPP(CHO), H ₂ TPP(CH ₂ OH) and H ₂ TPP(COOH) respectively. Color codes for atoms: C (grey), N (blue) and O (red).	5
Figure S2. UV-Visible spectra of 1 , 4 and 5 in CH ₂ Cl ₂ at 298 K.	7
Figure S3. UV-Visible spectra of 1 and 1d in CH ₂ Cl ₂ at 298 K.	7
Figure S4. UV-Visible spectra of 4 and 4d in CH ₂ Cl ₂ at 298 K.	8
Figure S5. UV-Visible spectra of 1d-5d in CH ₂ Cl ₂ at 298 K.	8
Figure S6. UV-Visible spectra of 1d-3d in CH ₂ Cl ₂ at 298 K.	9
Figure S7. UV-Visible spectra of 1d , 4d and 5d in CH ₂ Cl ₂ at 298 K.	9
Figure S8. Fluorescence spectra of 1-5 in CH ₂ Cl ₂ at 298 K.	11
Figure S9. Fluorescence spectra of 1a-5a in CH ₂ Cl ₂ at 298 K.	11
Figure S10. Fluorescence spectra of 1 and 1a in CH ₂ Cl ₂ at 298 K.	12
Figure S11. Fluorescence spectra of 4 and 4a in CH ₂ Cl ₂ at 298 K.	12
Figure S12. Fluorescence spectra of 5 and 5a in CH ₂ Cl ₂ at 298 K.	13
Figure S13. Fluorescence spectra of 3 and 3a in CH ₂ Cl ₂ at 298 K.	13
Figure S14. Fluorescence spectra of 2 and 2a in CH ₂ Cl ₂ at 298 K.	14
Figure S15. ¹ H NMR spectrum of 1 in CDCl ₃ at 298 K.	15

Figure S16. ^1H NMR spectrum of 1d in CDCl_3 at 298 K.	16
Figure S17. ^1H NMR spectrum of 4 in CDCl_3 at 298 K.	17
Figure S18. ^1H NMR spectrum of 4d in CDCl_3 at 298 K.	18
Figure S19. ^1H NMR spectrum of 5 in CDCl_3 at 298 K.	19
Figure S20. ^1H NMR spectrum of 5d in CDCl_3 at 298 K.	20
Figure S21. ^1H NMR spectrum of 3 in CDCl_3 at 298 K.	21
Figure S22. ^1H NMR spectrum of 3d in CDCl_3 at 298 K.	22
Figure S23. ^1H NMR spectrum of 2 in CDCl_3 at 298 K.	23
Figure S24. ^1H NMR spectrum of 2d in CDCl_3 at 298 K.	24
Figure S25. Cyclic voltammograms of (a) $\text{H}_2\text{TPP}(\text{X})\text{Y}_2$, (b) $\text{ZnTPP}(\text{X})\text{Y}_2$ (c) $\text{CoTPP}(\text{X})\text{Y}_2$ (d) $\text{NiTPP}(\text{X})\text{Y}_2$ (where $\text{X} = \text{CHO}, \text{COOH}, \text{CH}_2\text{OH}$ and $\text{Y} = \text{H}, \text{Br}, \text{Ph}$) complexes in CH_2Cl_2 .	25
Figure S26. Cyclic voltammograms of (a) $\text{MTPP}(\text{CHO})$, (b) $\text{MTPP}(\text{CHO})\text{Br}_2$, (c) $\text{MTPP}(\text{CHO})(\text{Ph})_2$ (d) $\text{MTPP}(\text{COOH})$, (e) $\text{MTPP}(\text{CH}_2\text{OH})$ (where $\text{M} = \text{2H}, \text{Zn}, \text{Cu}, \text{Co}, \text{Ni}$) complexes in CH_2Cl_2 .	26-27
Figure S27. The HOMO-LUMO variation of various Mixed β -substituted porphyrins: (a) $\text{H}_2\text{TPP}(\text{X})\text{Y}_2$ (b) $\text{ZnTPP}(\text{X})\text{Y}_2$ (c) $\text{CoTPP}(\text{X})\text{Y}_2$ (d) $\text{NiTPP}(\text{X})\text{Y}_2$ (where $\text{X} = \text{CHO}, \text{COOH}, \text{CH}_2\text{OH}$ and $\text{Y} = \text{H}, \text{Br}, \text{Ph}$)	28-31
Table S1. Selected bond lengths (\AA) and bond angles (deg) for the B3LYP/6-311g(d,p) optimised geometries of $\text{H}_2\text{TPP}(\text{X})\text{Y}_2$ ($\text{X} = \text{CHO}, \text{CH}_2\text{OH}$ and COOH , $\text{Y} = \text{Br}$ and Ph).	6
Table S2. UV-Vis spectral data of $\text{Cu}(\text{II})$, $\text{Co}(\text{II})$ and $\text{Ni}(\text{II})$ complexes of β -mono- and tri-substituted porphyrins in CH_2Cl_2 at 298 K.	10
Table S3. Fluorescence Spectral data of mono/tri- β -substituted porphyrins in CH_2Cl_2 at 298 K.	14
Table S4. Modulation of frontier and subfrontier orbitals of $\text{CuTPP}(\text{X})\text{Y}_2$ w.r.t CuTPP .	32
Table S5. Modulation of frontier and subfrontier orbitals of $\text{ZnTPP}(\text{X})\text{Y}_2$ w.r.t ZnTPP .	32
Table S6. Modulation of frontier and subfrontier orbitals of $\text{CoTPP}(\text{X})\text{Y}_2$ w.r.t CoTPP .	33

CoTPP.



Scheme S1. Synthetic scheme for MTPP(X)Y₂.

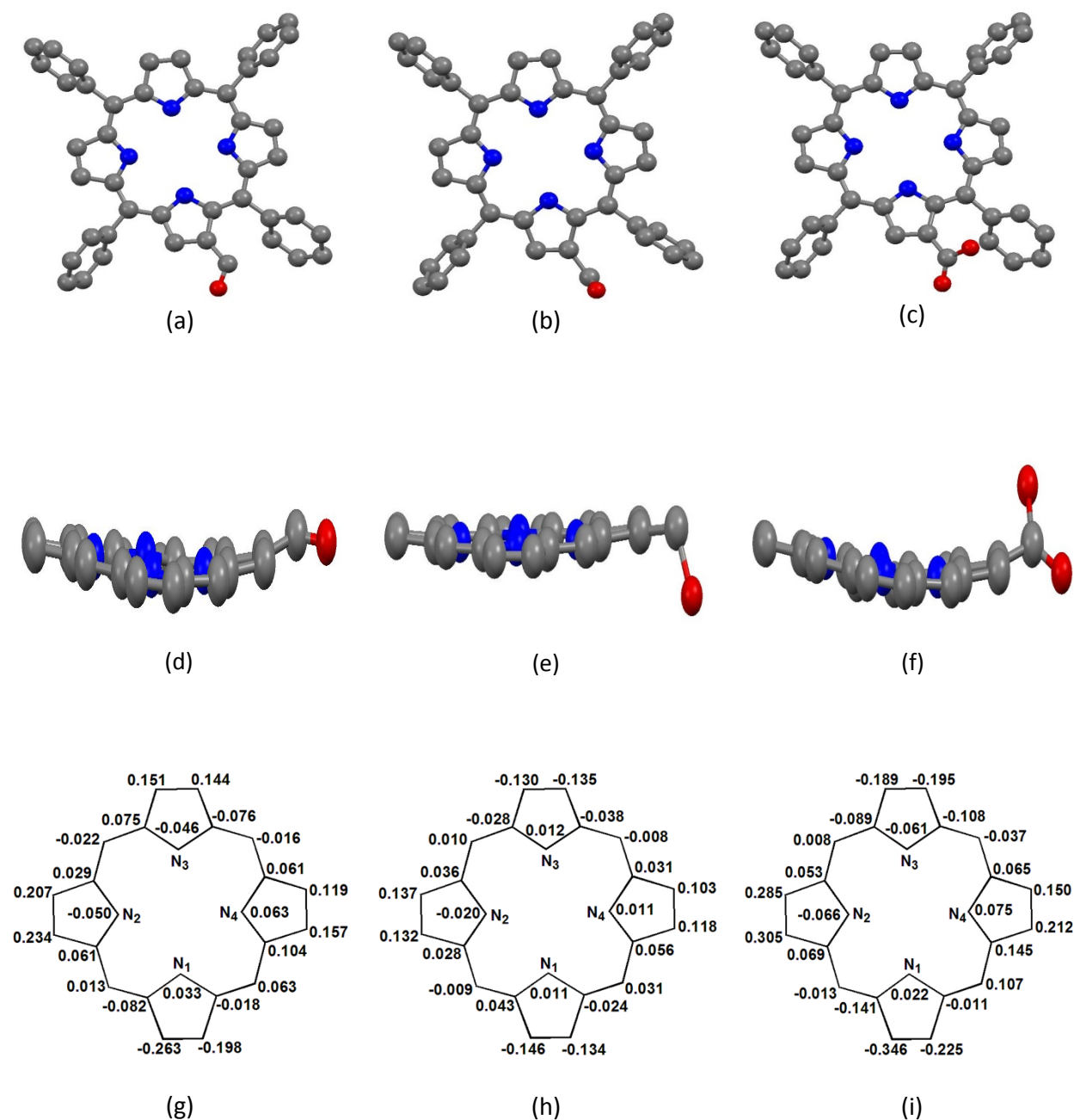


Figure S1. B3LYP/ 6-311g(d,p) optimised geometries showing top as well as side views of $\text{H}_2\text{TPP}(\text{CHO})$ (a and d), $\text{H}_2\text{TPP}(\text{CH}_2\text{OH})$ (b and e) and $\text{H}_2\text{TPP}(\text{COOH})$ (c and f), respectively. In side view, the β -substituents and *meso*-phenyl groups are not shown for clarity. The displacement of porphyrin-core atoms in Å from the mean plane are shown in figures g, h and i for $\text{H}_2\text{TPP}(\text{CHO})$, $\text{H}_2\text{TPP}(\text{CH}_2\text{OH})$ and $\text{H}_2\text{TPP}(\text{COOH})$ respectively. Color codes for atoms: C (grey), N (blue) and O (red).

Table S1. Selected bond lengths (Å) and bond angles (deg) for the B3LYP/6-311g(d,p) optimised geometries of H₂TPP(X)Y₂ (X = CHO, CH₂OH and COOH, Y = Br and Ph).

	H ₂ TPP(CHO)	H ₂ TPP(CH ₂ OH)	H ₂ TPP(COOH)	H ₂ TPP(CHO)Br ₂	H ₂ TPP(CHO)(Ph) ₂
Bond Length (Å)					
N-C _α	1.363	1.364	1.363	1.363	1.362
N'-C _{α'}	1.374	1.374	1.374	1.375	1.375
C _α -C _β	1.461	1.461	1.460	1.462	1.465
C _{α'} -C _{β'}	1.433	1.433	1.434	1.433	1.433
C_β-C_β	1.357	1.353	1.358	1.363	1.366
C _{β'} -C _{β'}	1.366	1.366	1.366	1.365	1.366
C _α -C _m	1.410	1.409	1.410	1.414	1.414
C _{α'} -C _m	1.401	1.402	1.402	1.403	1.403
ΔC_β (Å)^a	0.184	0.129	0.238	0.575	0.578
Δ24 (Å)^b	0.095	0.059	0.123	0.266	0.256
Bond Angle (deg)					
N-C_α-C_m	125.78	125.59	125.83	124.52	124.49
N'-C _{α'} -C _m	126.94	127.06	127.00	127.19	126.81
N-C _α -C _β	110.64	110.62	110.54	109.91	110.59
N'-C _{α'} -C _{β'}	106.45	106.43	106.43	106.29	106.28
C_β-C_α-C_m	123.54	123.74	123.52	125.47	124.98
C _{β'} -C _{α'} -C _m	126.58	126.49	126.68	126.46	126.70
C _α -C _β -C _β	106.34	106.38	106.38	106.46	106.73
C _{α'} -C _{β'} -C _{β'}	108.19	108.20	108.20	108.26	108.26
C _α -N-C _α	105.99	105.80	106.08	107.00	106.32
C _{α'} -N-C _{α'}	110.69	110.72	110.71	110.83	110.88
C _α -C _m -C _{α'}	125.36	125.66	125.18	124.73	124.70

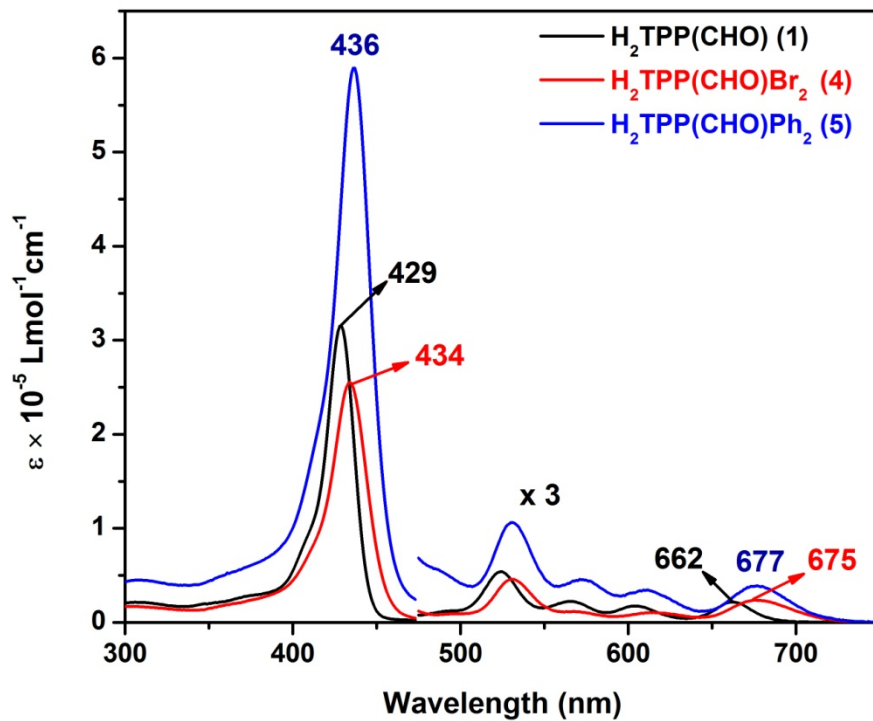


Figure S2. UV-Visible spectra of **1**, **4** and **5** in CH_2Cl_2 at 298 K.

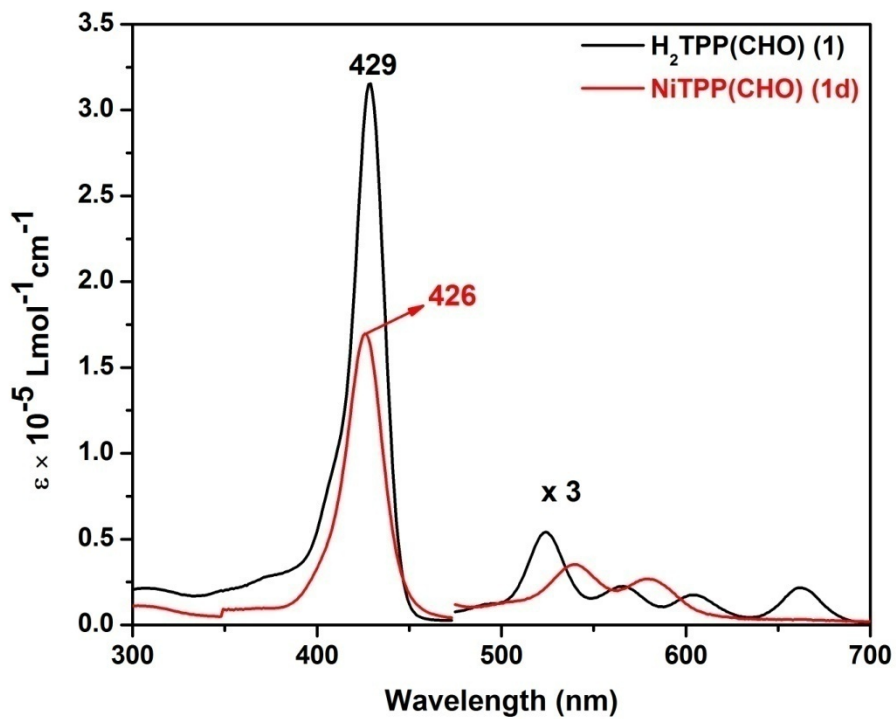


Figure S3. UV-Visible spectra of **1** and **1d** in CH_2Cl_2 at 298 K.

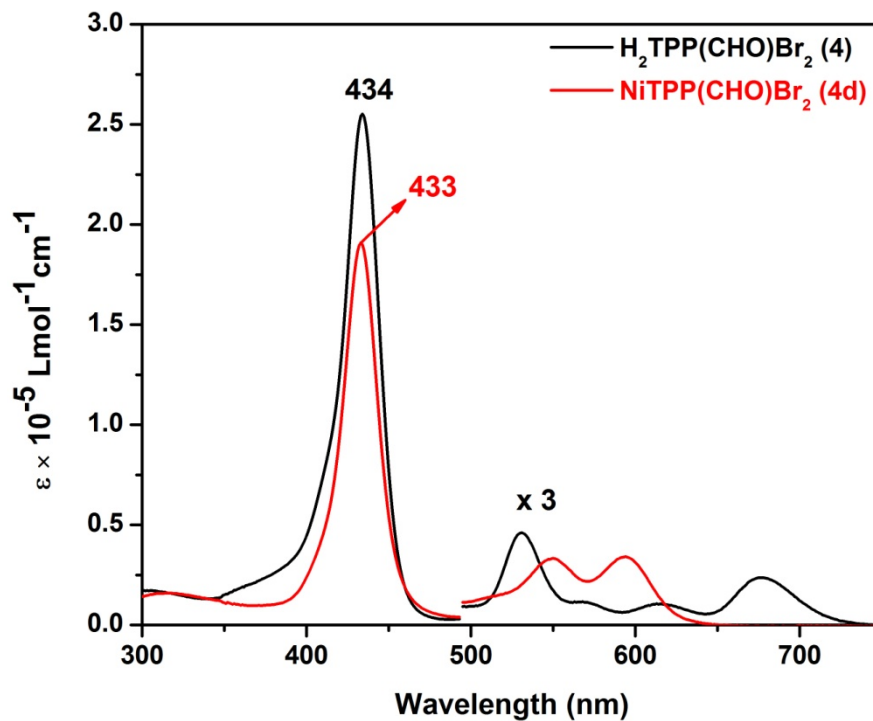


Figure S4. UV-Visible spectra of **4** and **4d** in CH_2Cl_2 at 298 K.

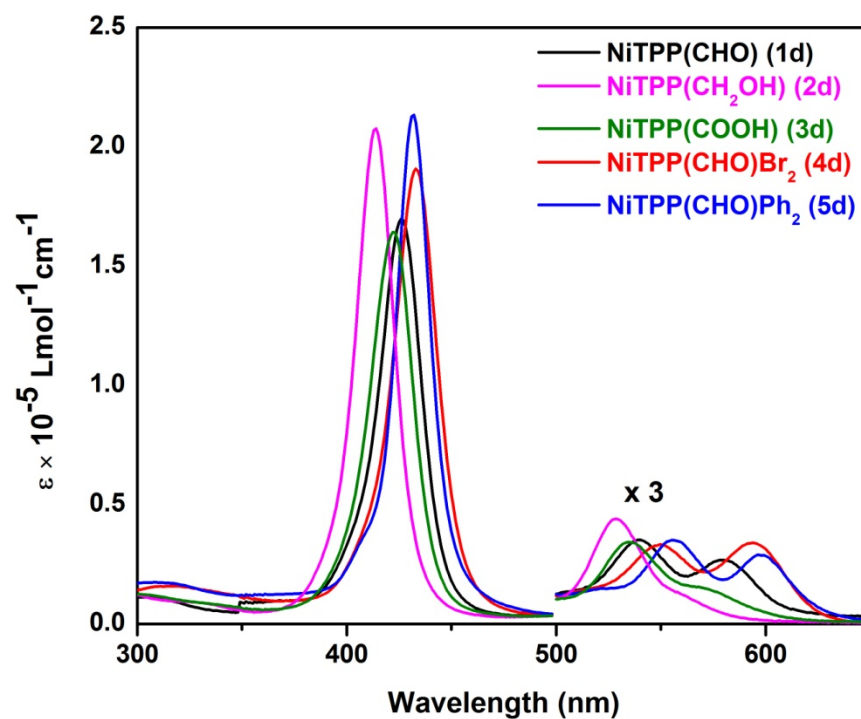


Figure S5. UV-Visible spectra of **1d** - **5d** in CH_2Cl_2 at 298 K.

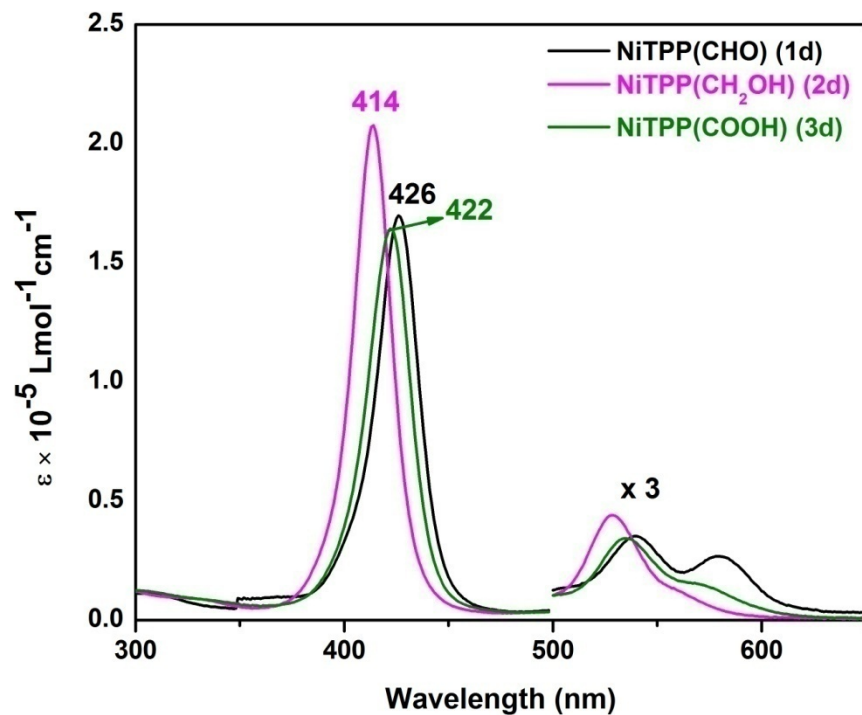


Figure S6. UV-Visible spectra of **1d** - **3d** in CH₂Cl₂ at 298 K.

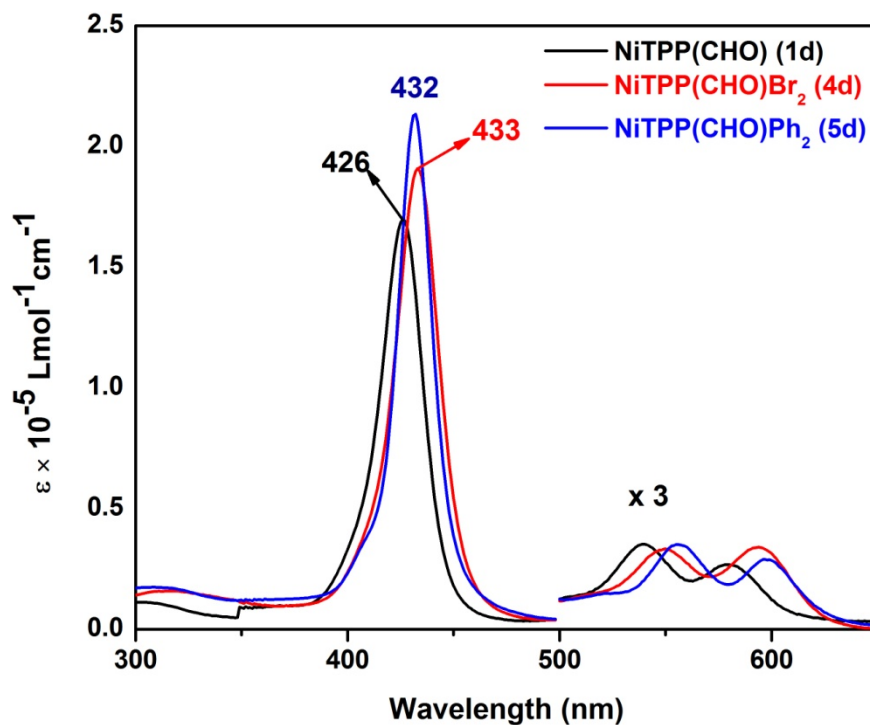


Figure S7. UV-Visible spectra of **1d**, **4d** and **5d** in CH₂Cl₂ at 298 K.

Table S2. UV-Vis spectral data of Cu(II), Co(II) and Ni(II) complexes of β -mono- and trisubstituted porphyrins in CH₂Cl₂ at 298 K.

Porphyrin	B band, λ_{\max},nm	Q bands, λ_{\max}, nm
CuTPP(CHO) (1b)	426(5.33)	549(3.97),591(3.79)
CuTPP(CH ₂ OH) (2b)	414(5.59)	538(4.23)
CuTPP(COOH) (3b)	421(5.48)	545(4.22),581(3.68)
CuTPPBr ₂ (CHO) (4b)	430(5.31)	557(3.98),598(3.95)
CuTPP(Ph ₂)(CHO) (5b)	432(5.33)	556(4.04),597(3.97)
CoTPP(CHO) (1c)	422(4.80)	539(3.51),577(3.38)
CoTPP(CH ₂ OH) (2c)	409(5.38)	528(4.14)
CoTPP(COOH) (3c)	416(5.23)	535(4.04)
CoTPPBr ₂ (CHO) (4c)	428(5.18)	549(3.98),589(4.0)
CoTPP(Ph ₂)(CHO) (5c)	429(4.96)	550(3.81),587(3.80)
NiTPP(CHO) (1d)	426(5.22)	540(4.06),580(3.94)
NiTPP(CH ₂ OH) (2d)	414(5.31)	529(4.16)
NiTPP(COOH) (3d)	422(5.21)	535(4.05),561(sh)
NiTPPBr ₂ (CHO) (4d)	430(5.27)	550(4.03),594(4.04)
NiTPP(Ph ₂)(CHO) (5d)	432(5.32)	556(4.06),596(3.98)

^aThe values in parentheses refer to log ϵ values, ϵ in dm³/mol/cm; Por = Porphyrin; sh = shoulder.

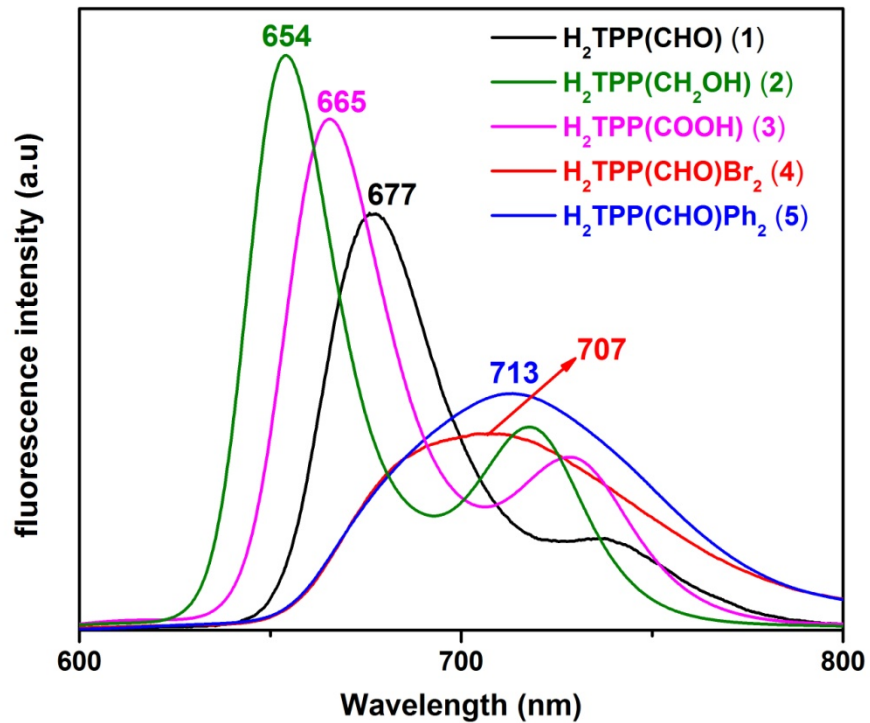


Figure S8. Fluorescence spectra of **1** - **5** in CH_2Cl_2 at 298 K.

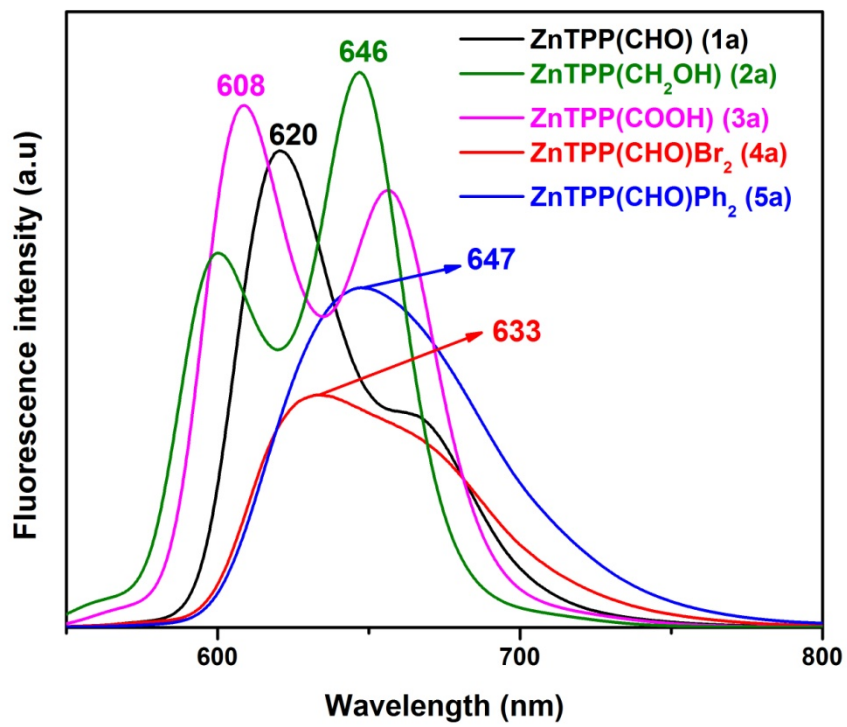


Figure S9. Fluorescence spectra of **1a** - **5a** in CH₂Cl₂ at 298 K.

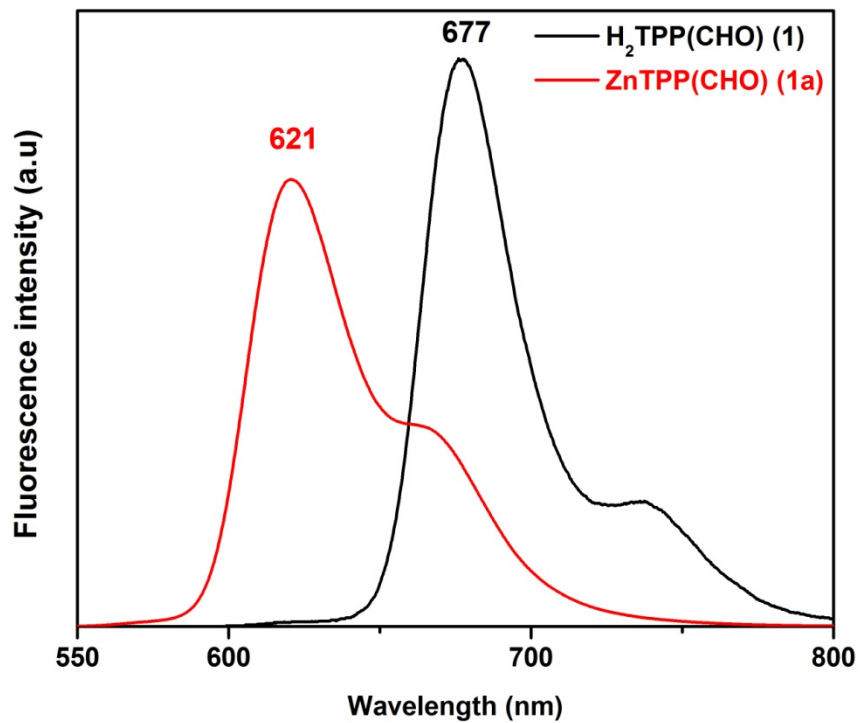


Figure S10. Fluorescence spectra of **1** and **1a** in CH₂Cl₂ at 298 K.

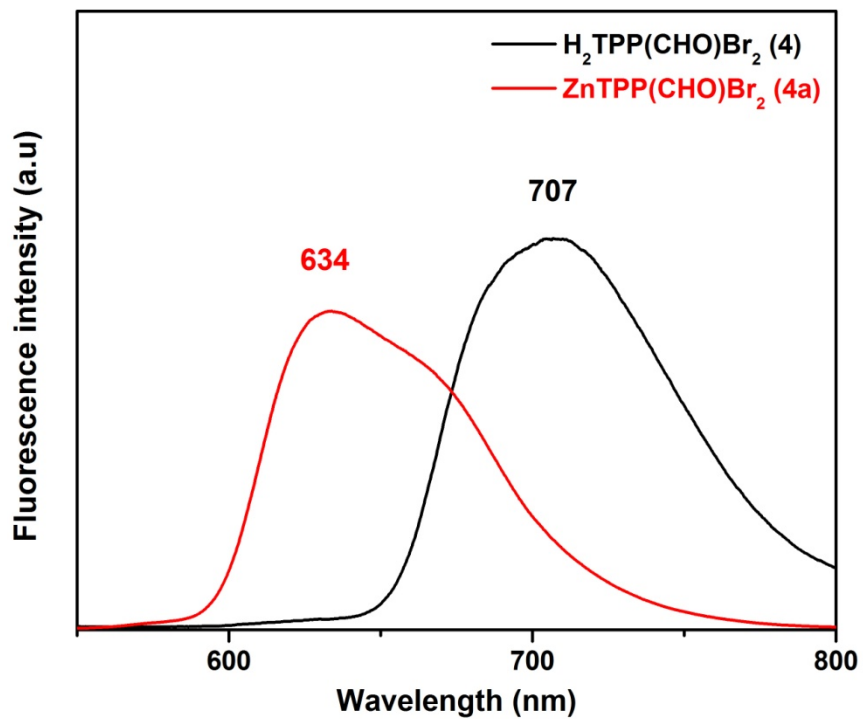


Figure S11. Fluorescence spectra of **4** and **4a** in CH₂Cl₂ at 298 K.

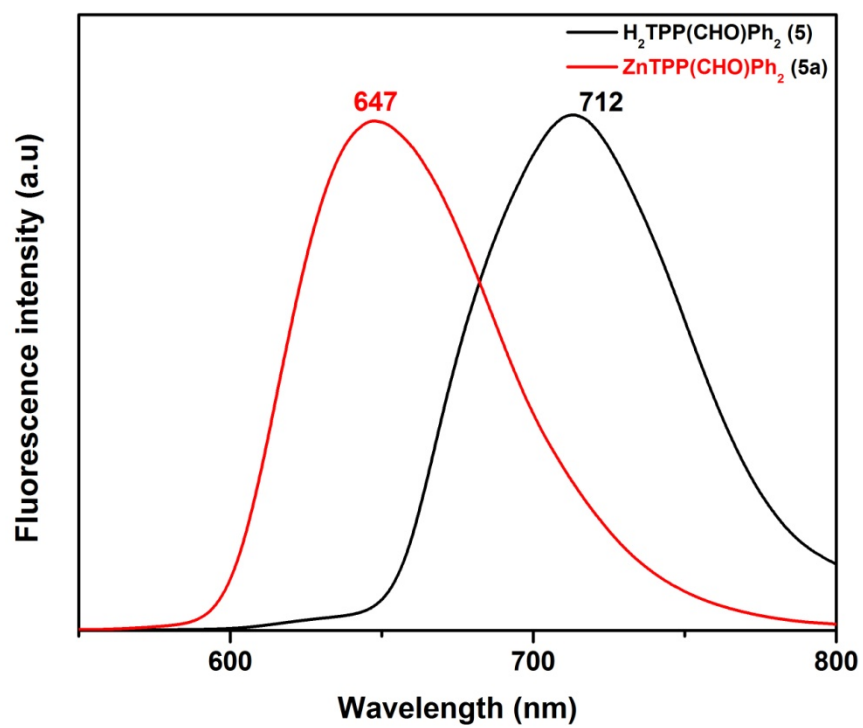


Figure S12. Fluorescence spectra of **5** and **5a** in CH₂Cl₂ at 298 K.

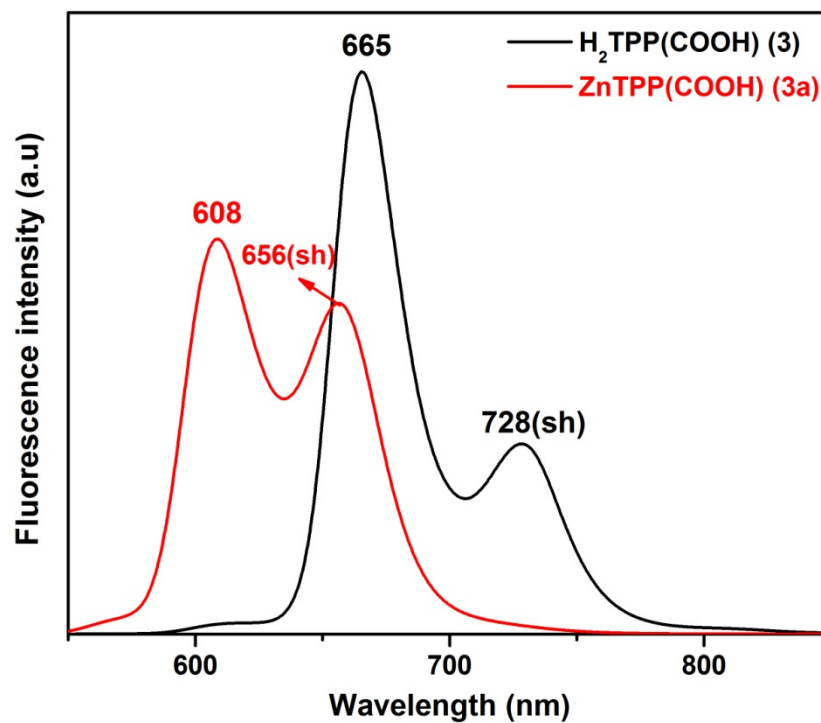


Figure S13. Fluorescence spectra of **3** and **3a** in CH₂Cl₂ at 298 K.

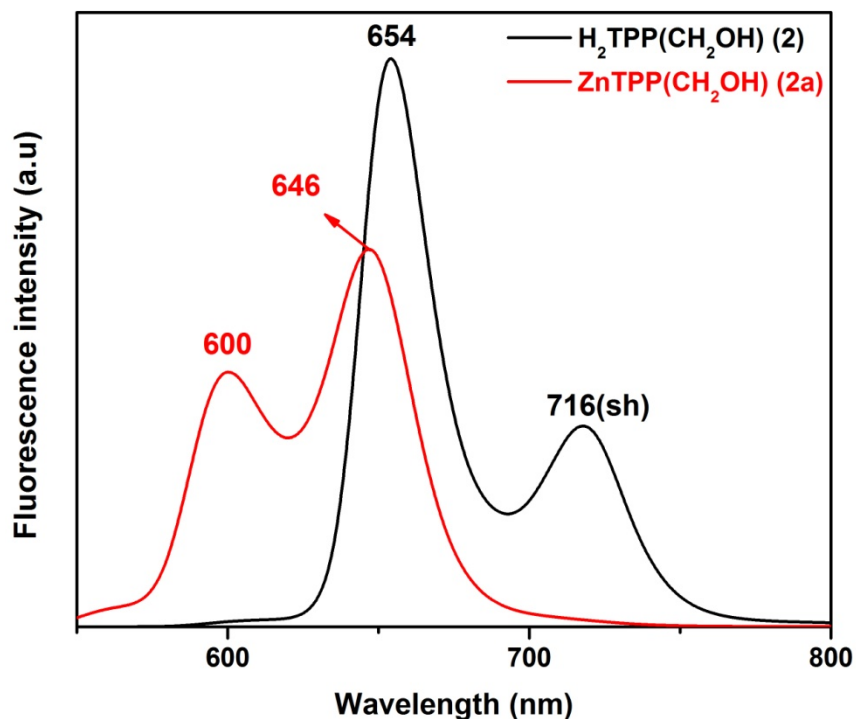


Figure S14. Fluorescence spectra of **2** and **2a** in CH₂Cl₂ at 298 K.

Table S3. Fluorescence Spectral data of mono/tri- β -substituted porphyrins in CH₂Cl₂ at 298 K.

Porphyrin	λ_{Ex} nm	$\lambda_{\text{fl,max}}$ nm	Quantum Yield, ϕ_f^a	Stokes shift (nm)	Stokes shift (cm ⁻¹)
1	429	677	0.1420 \pm 0.0030	15	334
2	417	654	0.1132 \pm 0.0020	9	213
3	423	665	0.0913 \pm 0.0021	13	300
4	434	707	0.0025 \pm 0.0003	32	670
5	436	713	0.0560 \pm 0.0018	36	746
1a	430	620	0.0209 \pm 0.0011	19	509
2a	418	606	0.0266 \pm 0.0013	53	1615
3a	425	608	0.0279 \pm 0.0009	16	444
4a	434	633	0.0009 \pm 0.00001	27	704
5a	436	647	0.0091 \pm 0.0004	41	1046

^a ϕ_f were calculated using literature method (E. Austin and M. Gouterman, *Bioinorg. Chem.* 1978, **9**, 281).

Fluorescence quantum yield are determined by the comparative method.¹⁻²

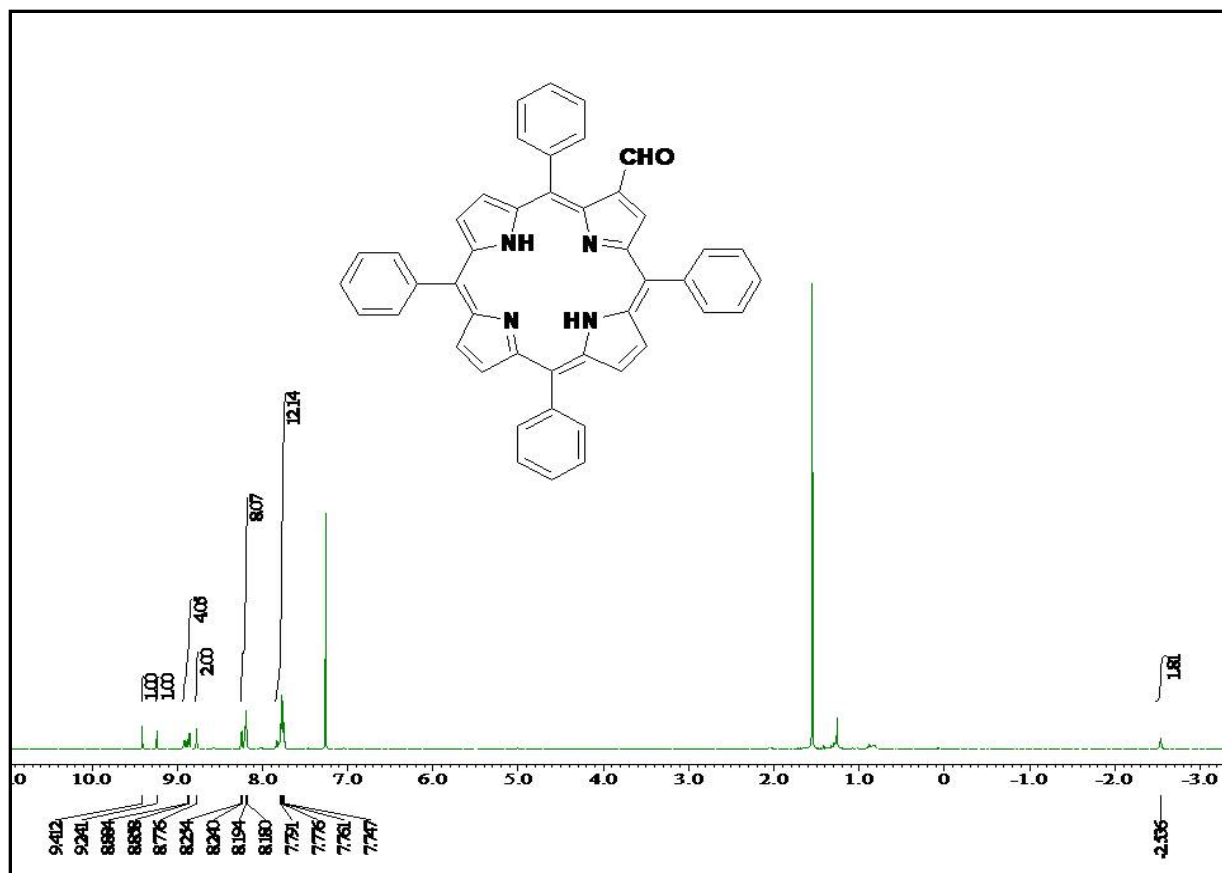


Figure S15. ¹H NMR spectrum of **1** in CDCl₃ at 298 K.

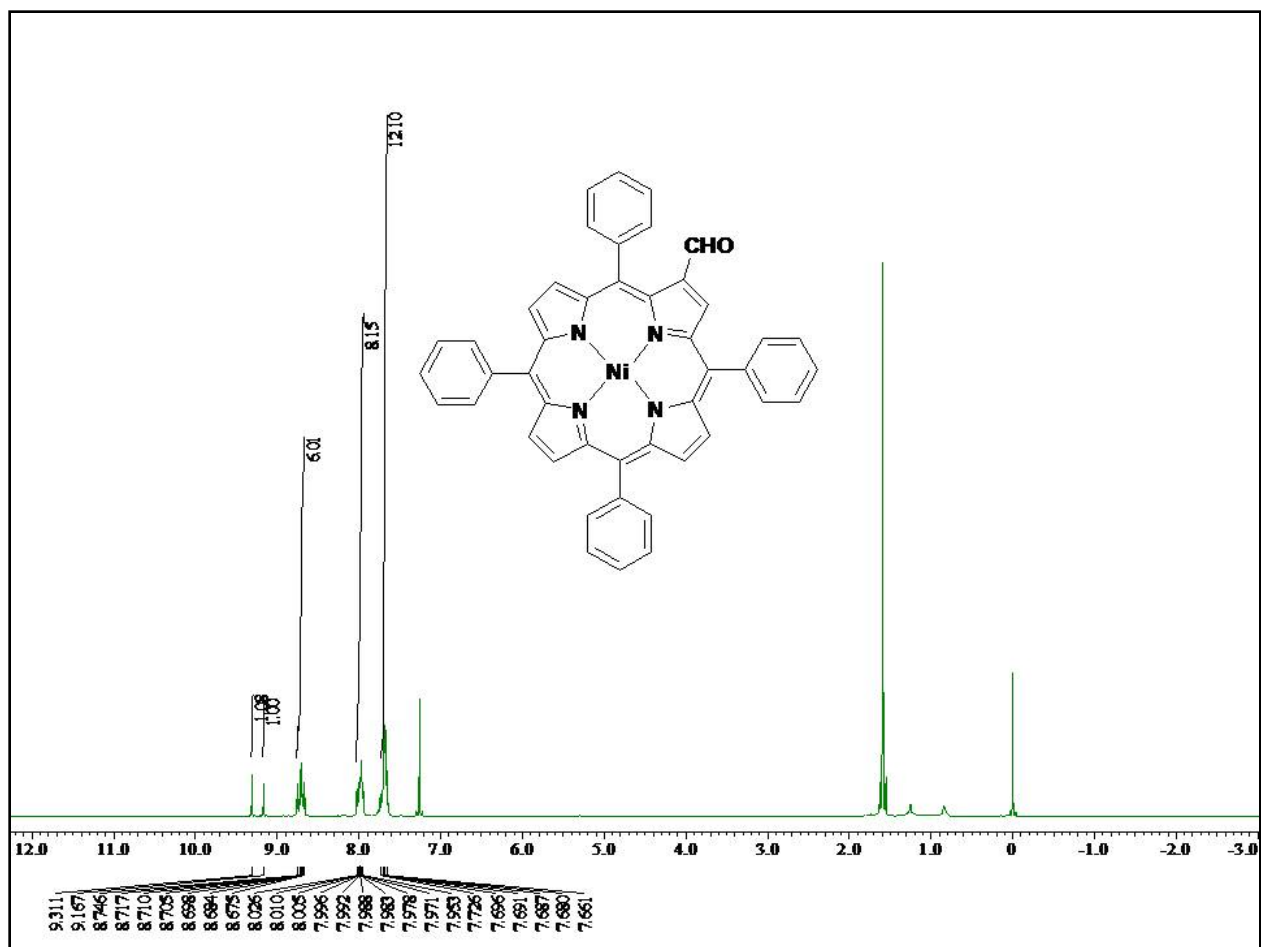


Figure S16. ¹H NMR spectrum of **1d** in CDCl₃ at 298 K.

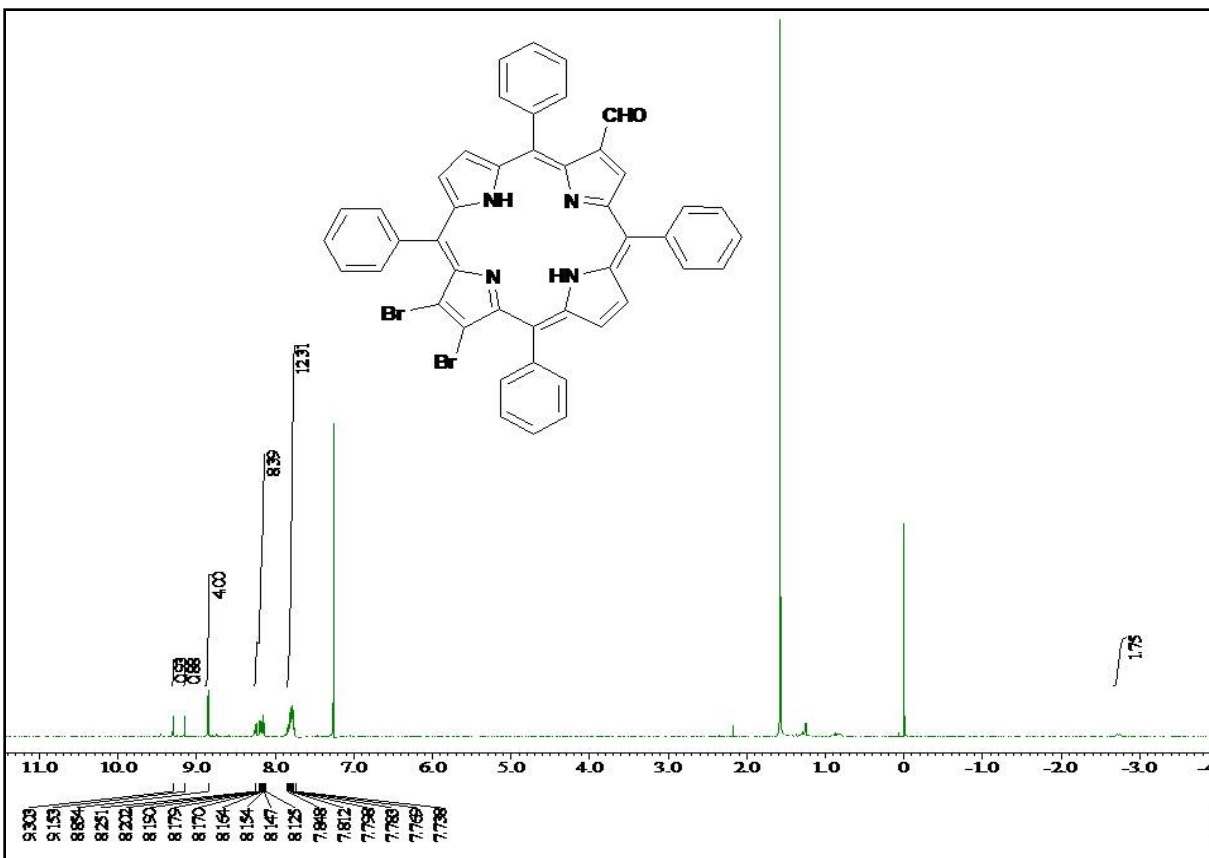


Figure S17. ¹H NMR spectrum of 4 in CDCl₃ at 298 K.

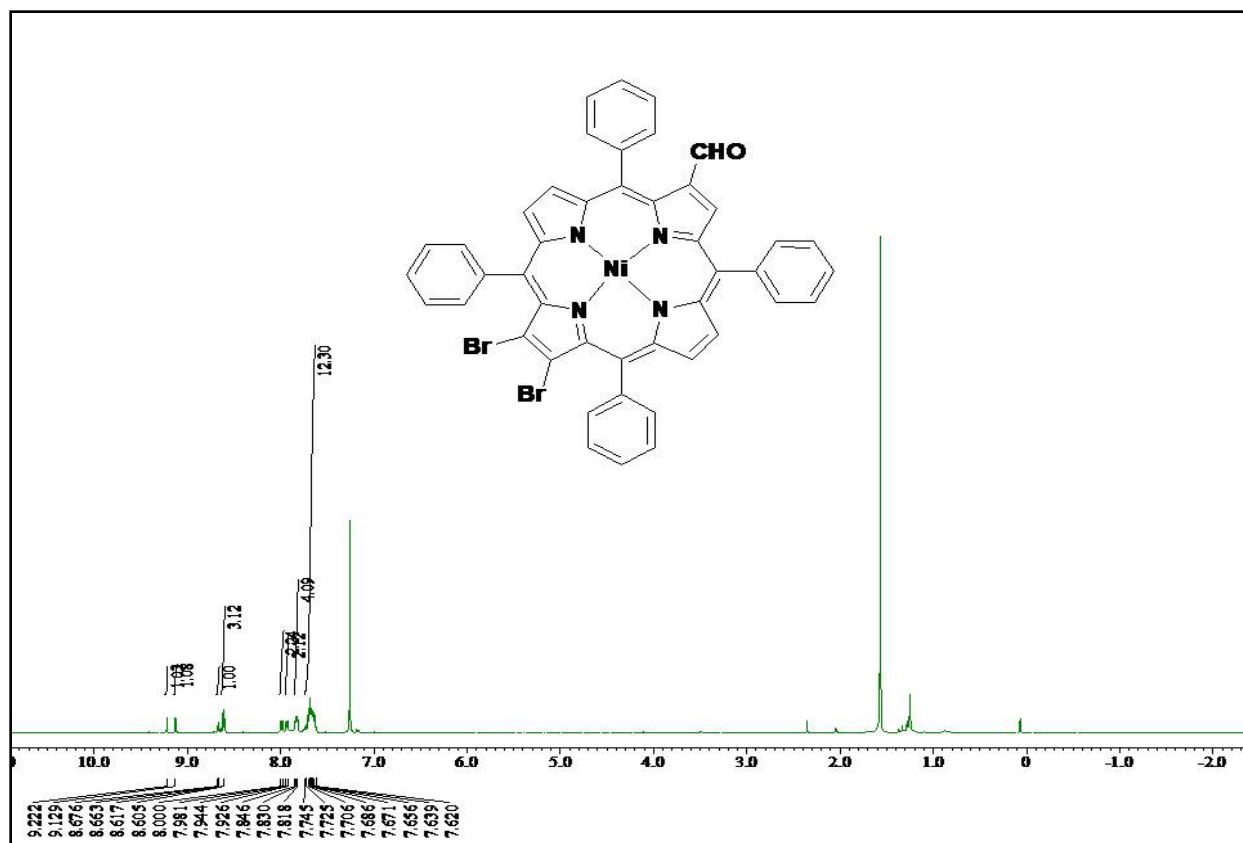


Figure S18. ^1H NMR spectrum of **4d** in CDCl_3 at 298 K.

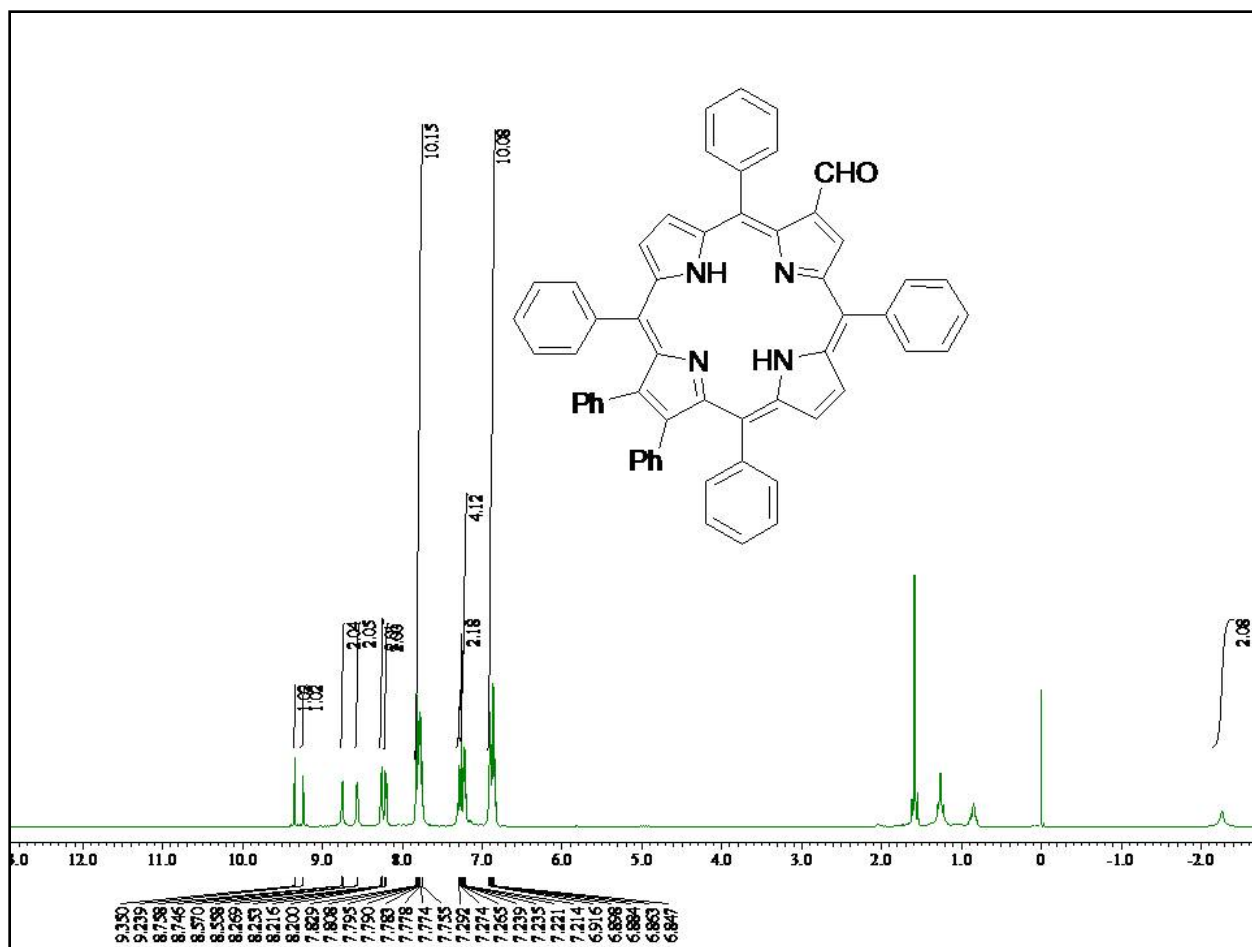


Figure S19. ^1H NMR spectrum of **5** in CDCl_3 at 298 K.

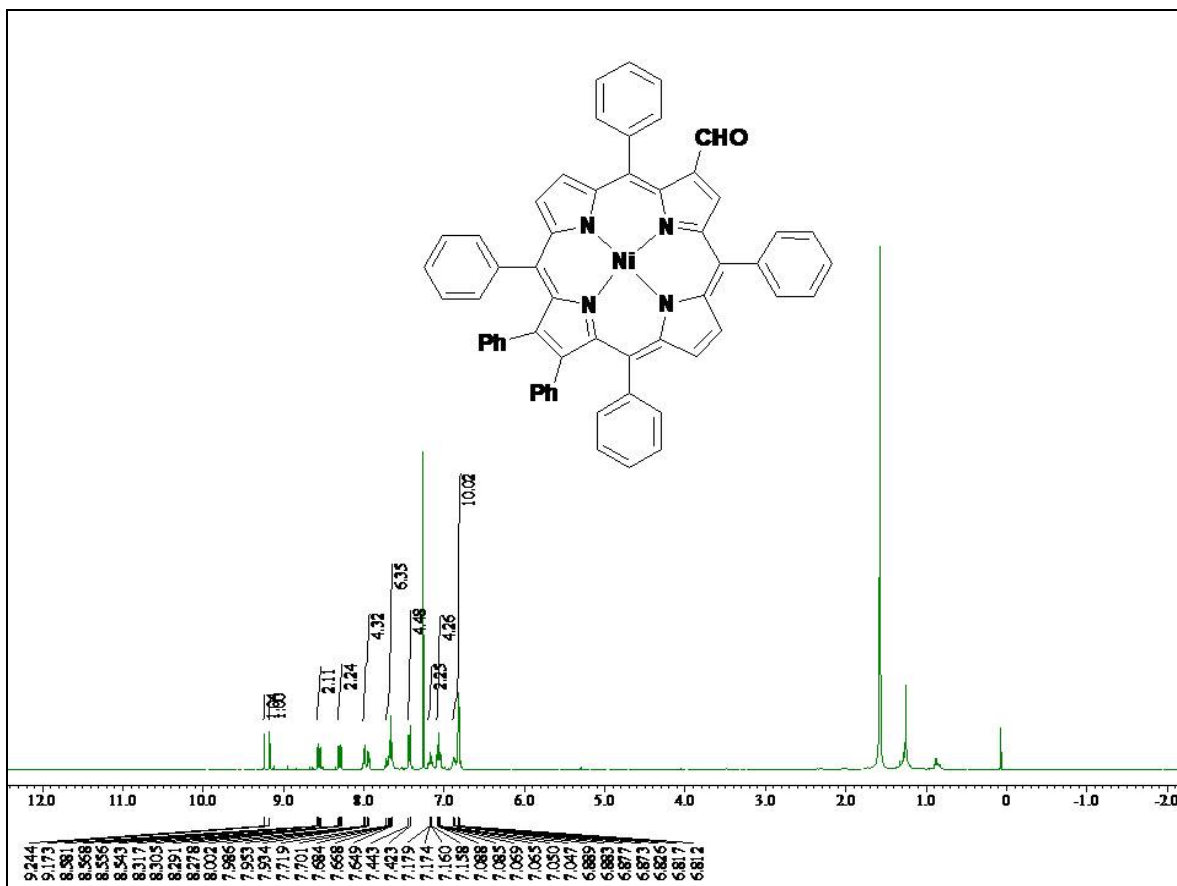


Figure S20. ¹H NMR spectrum of **5d** in CDCl₃ at 298 K.

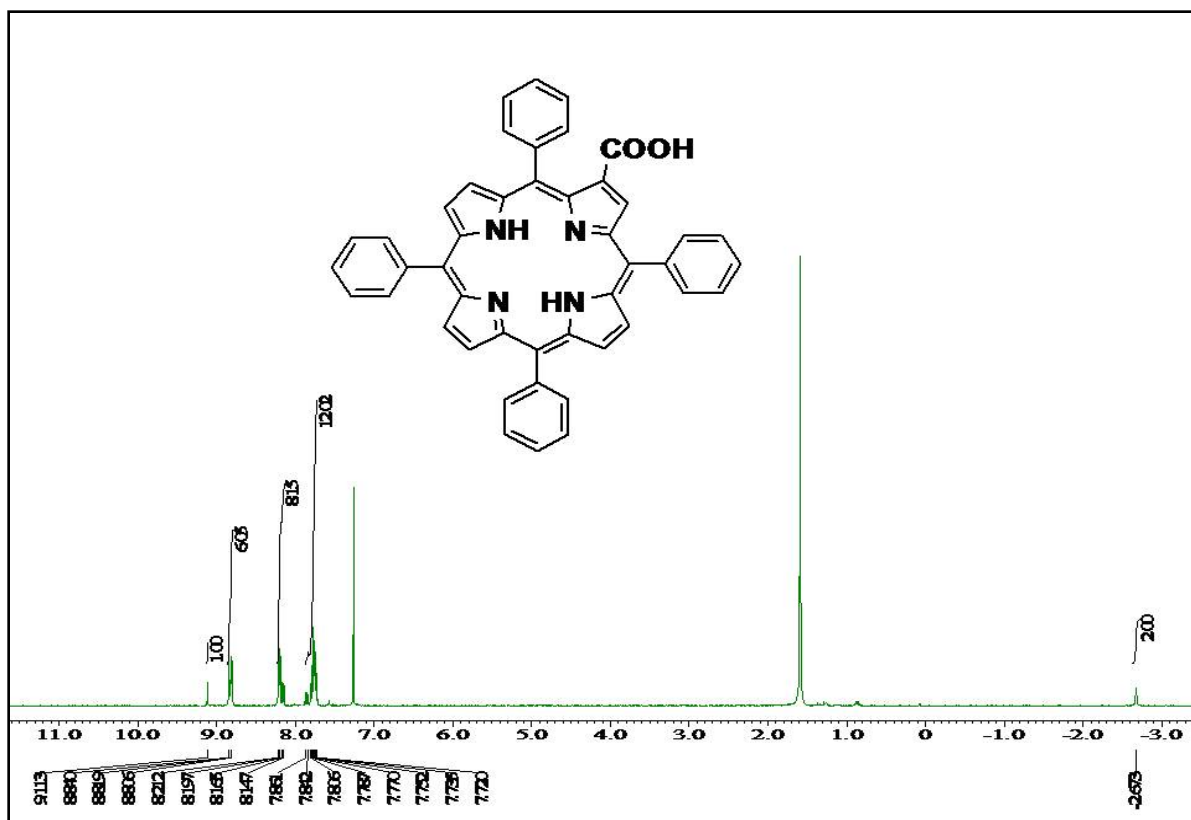


Figure S21. ¹H NMR spectrum of **3** in CDCl₃ at 298 K

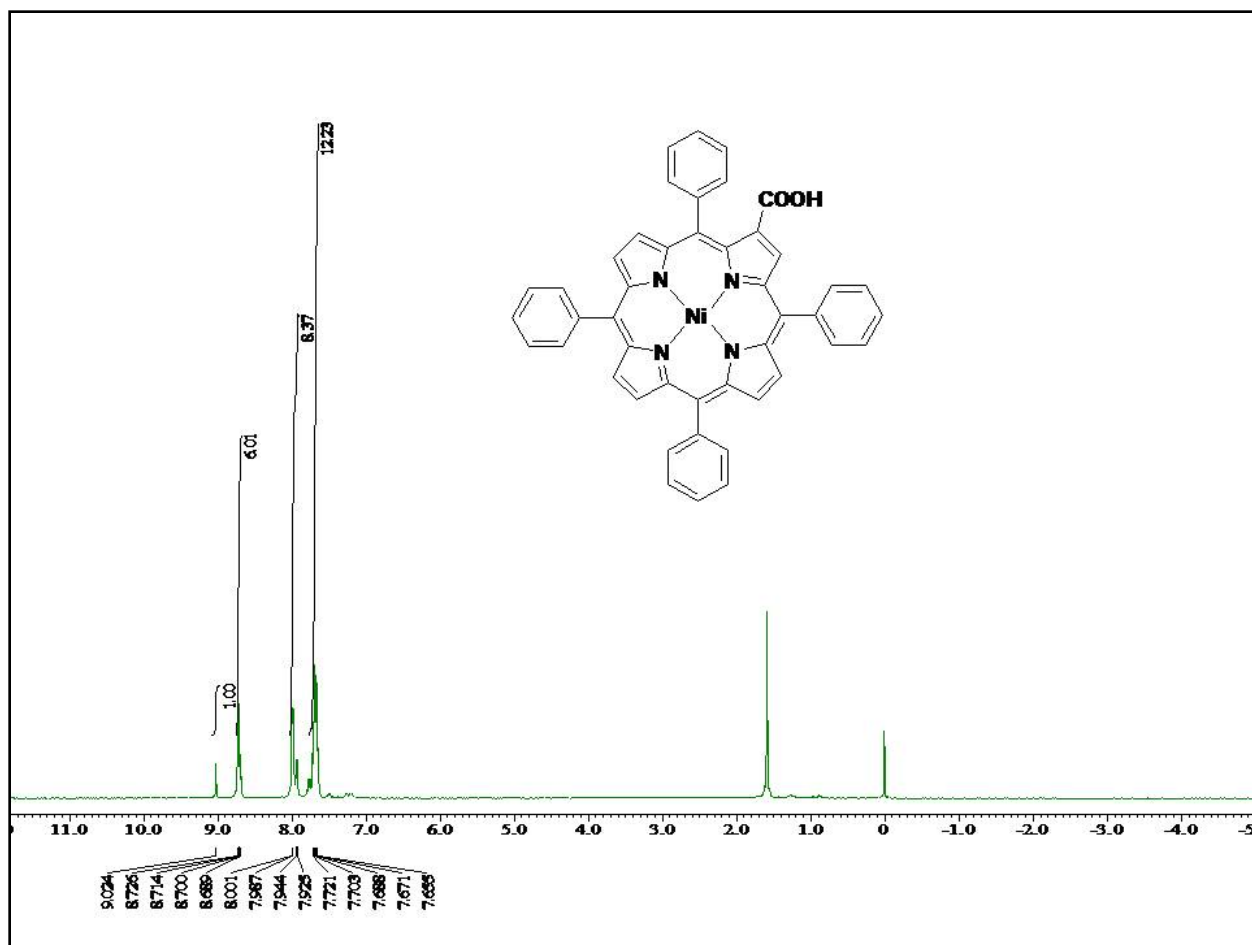


Figure S22. ¹H NMR spectrum of **3d** in CDCl₃ at 298 K.

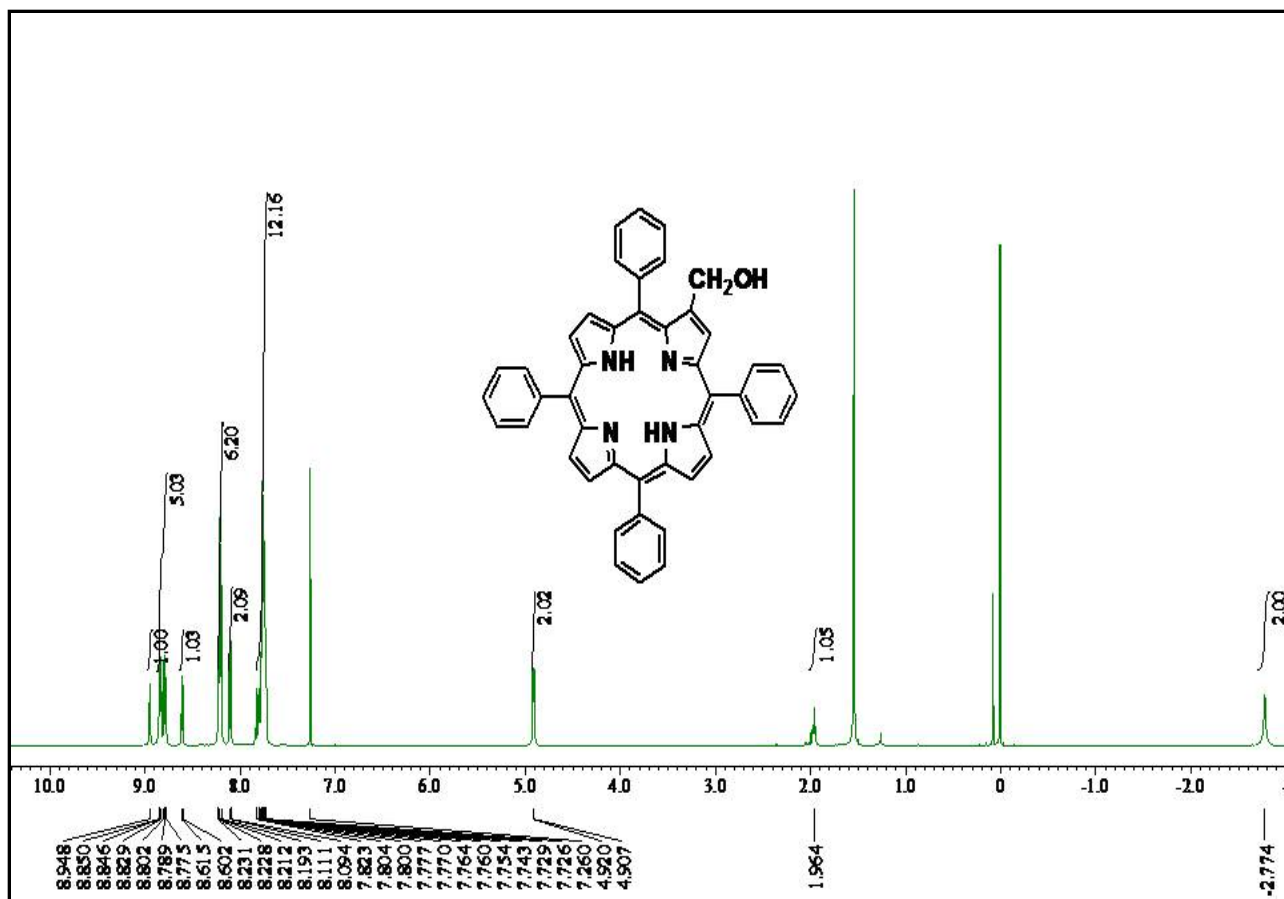


Figure S23. ^1H NMR spectrum of **2** in CDCl_3 at 298 K

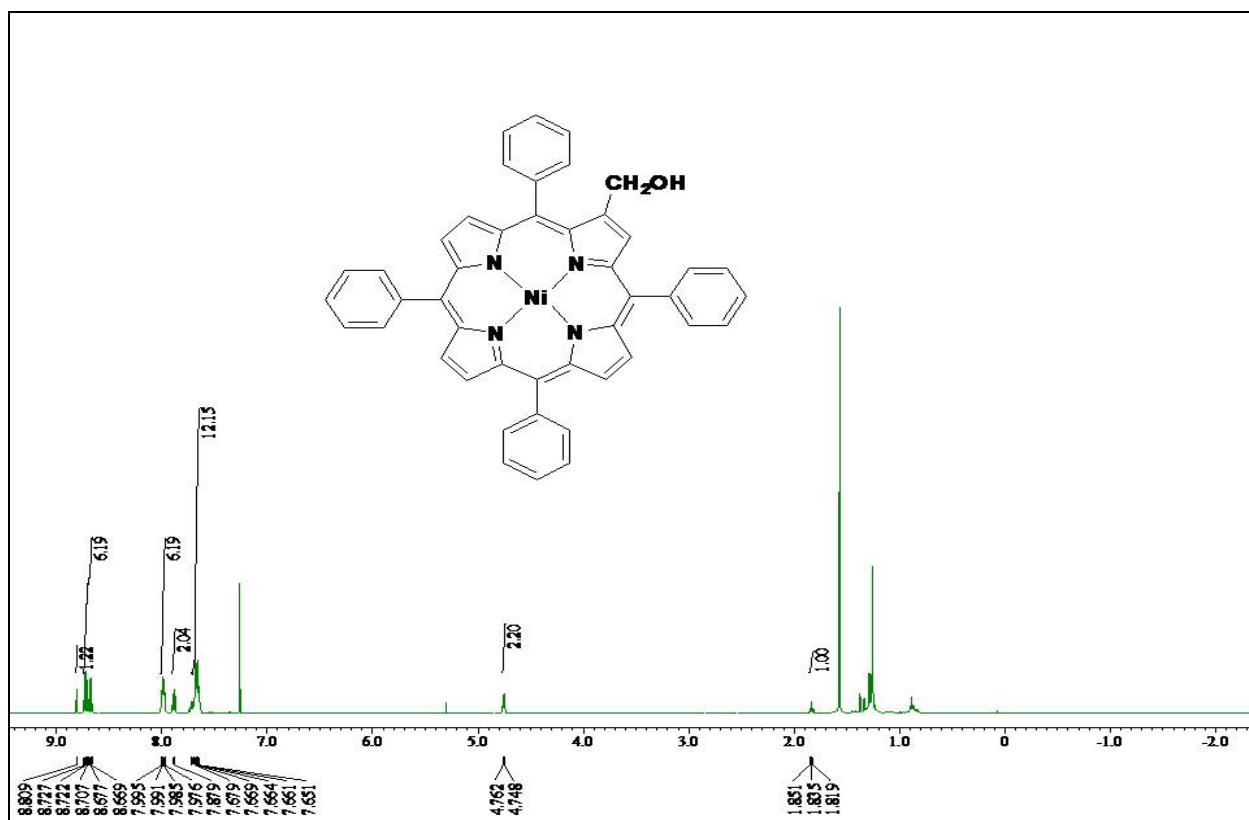


Figure S24. ^1H NMR spectrum of **2d** in CDCl_3 at 298 K.

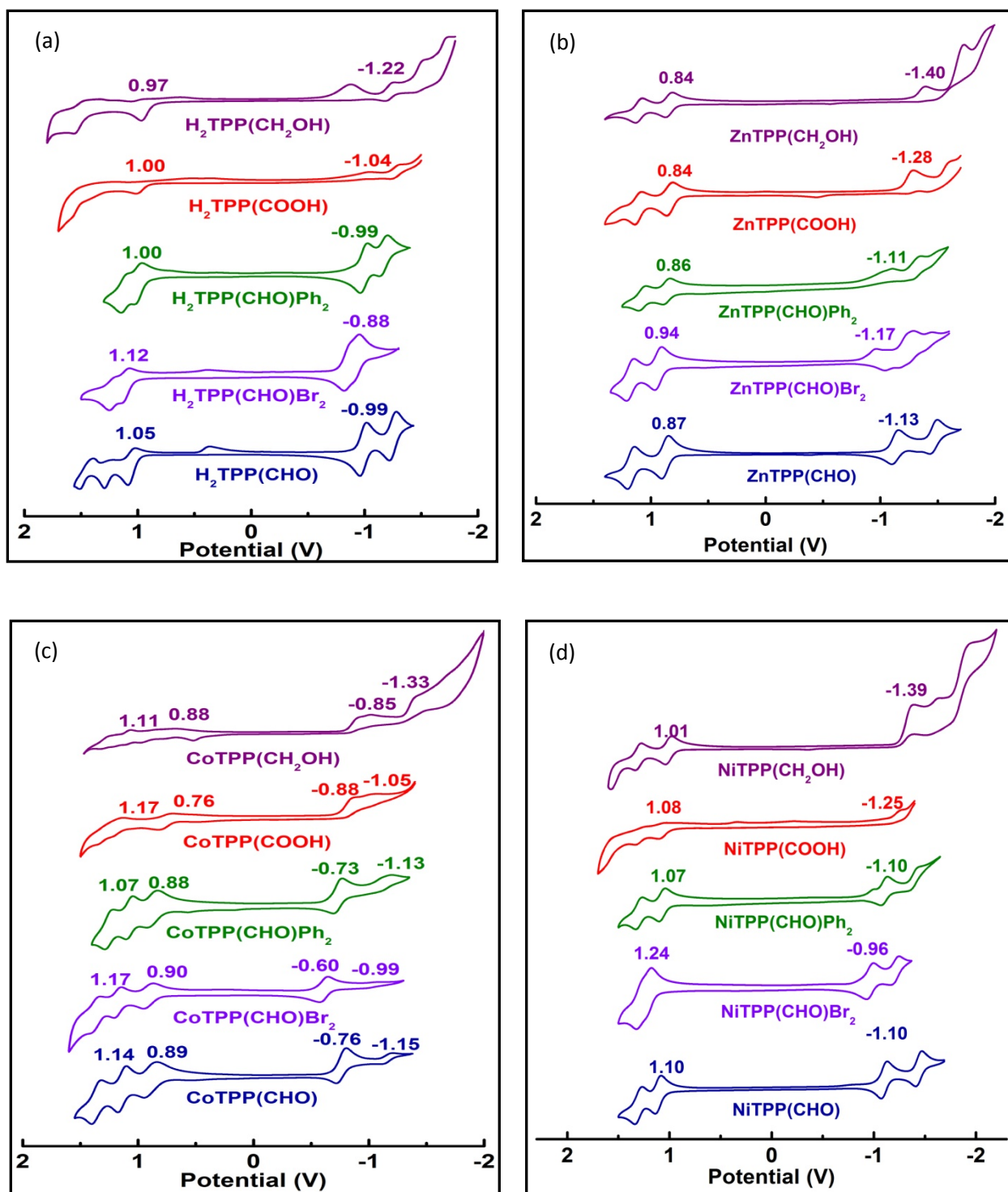
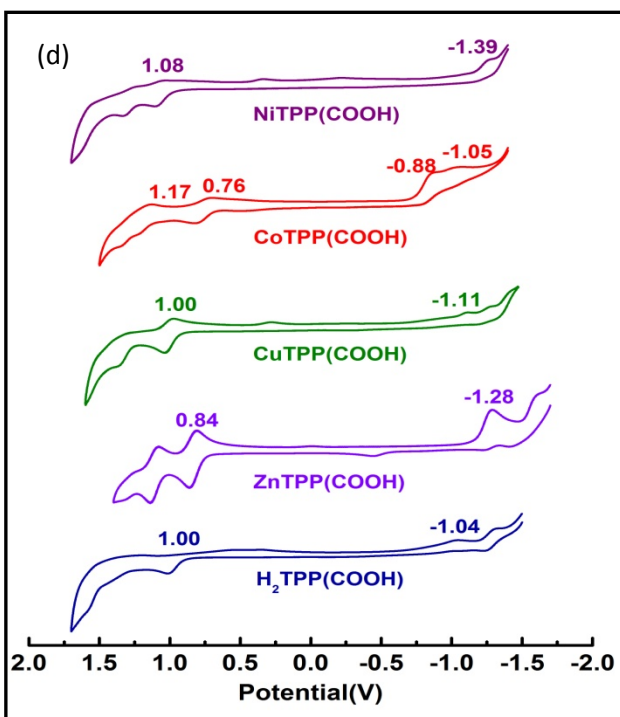
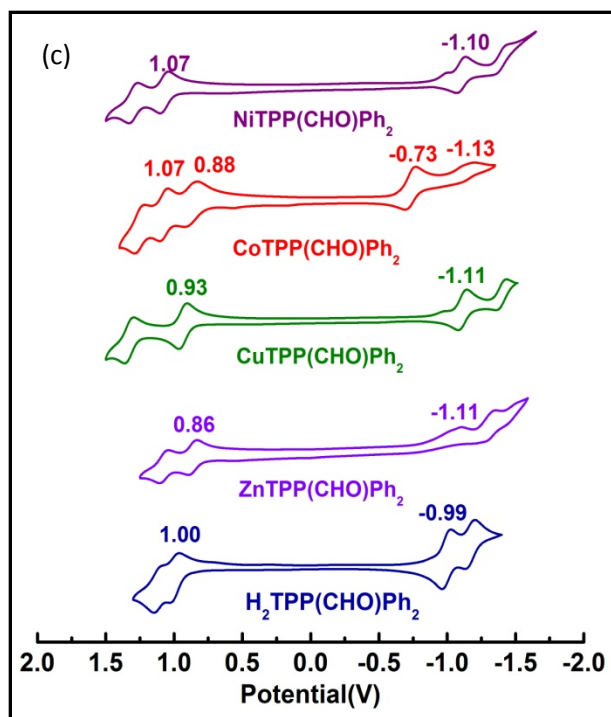
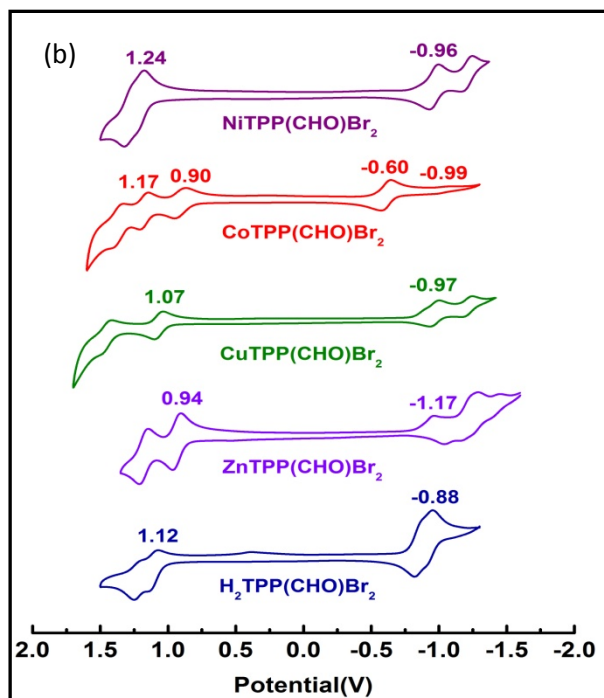
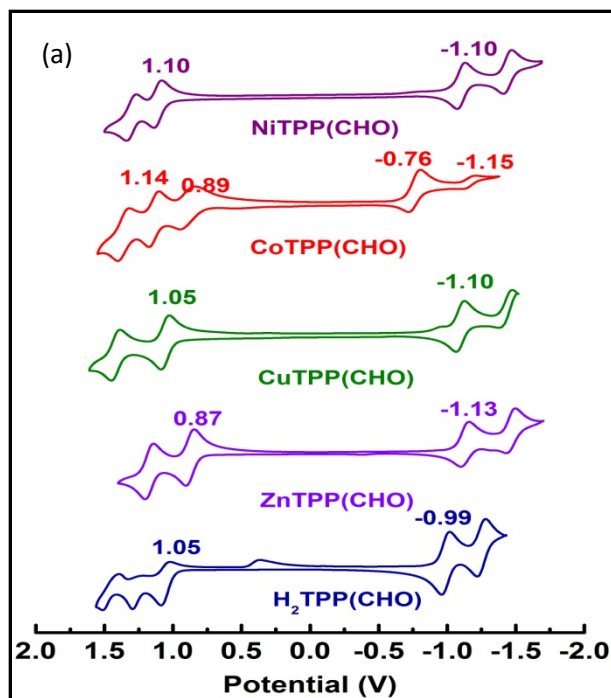


Figure S25. Cyclic voltammograms of (a) $\text{H}_2\text{TPP}(\text{X})\text{Y}_2$, (b) $\text{ZnTPP}(\text{X})\text{Y}_2$ (c) $\text{CoTPP}(\text{X})\text{Y}_2$ (d) $\text{NiTPP}(\text{X})\text{Y}_2$ (where X = CHO, COOH, CH_2OH and Y = H, Br, Ph) complexes in CH_2Cl_2 .



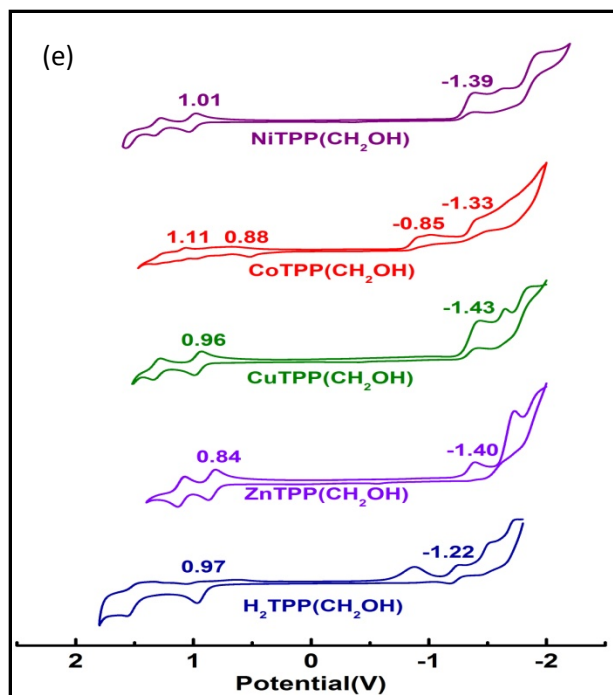
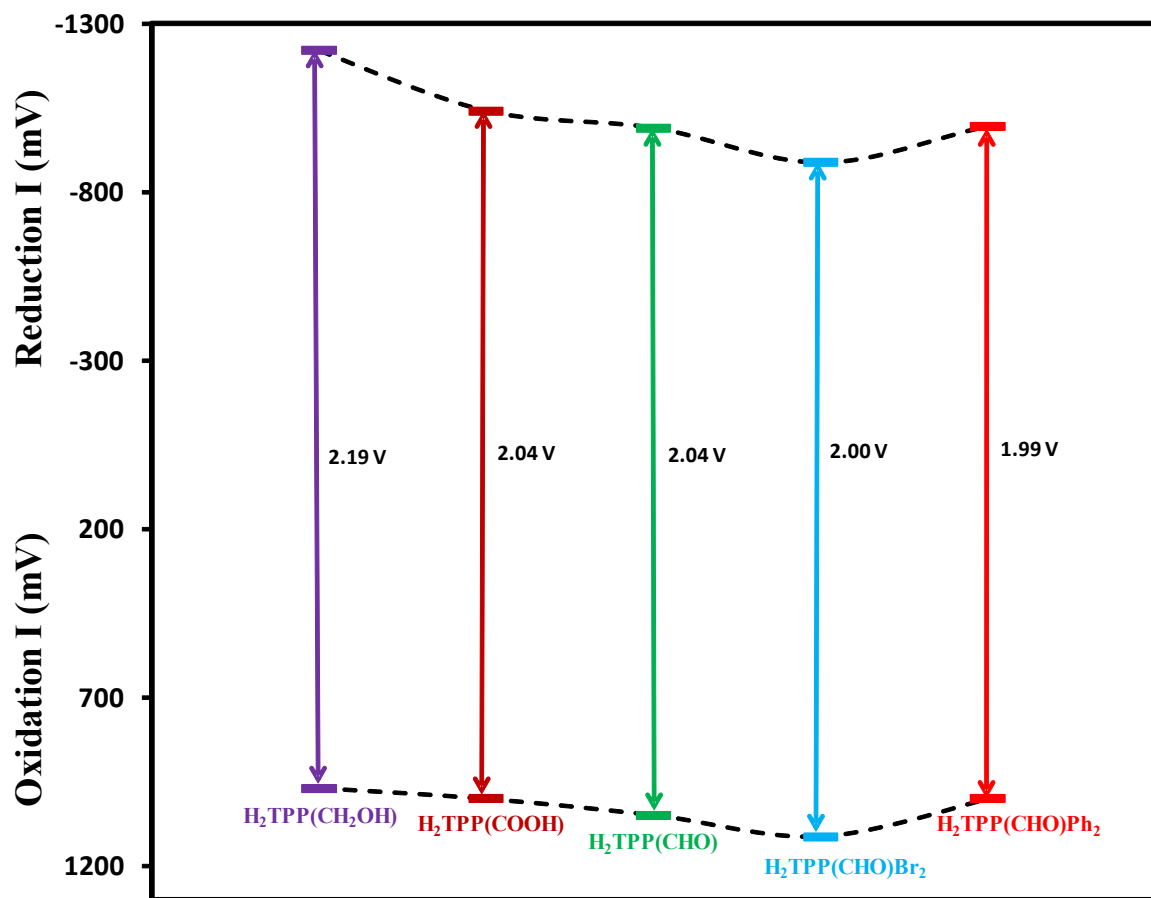
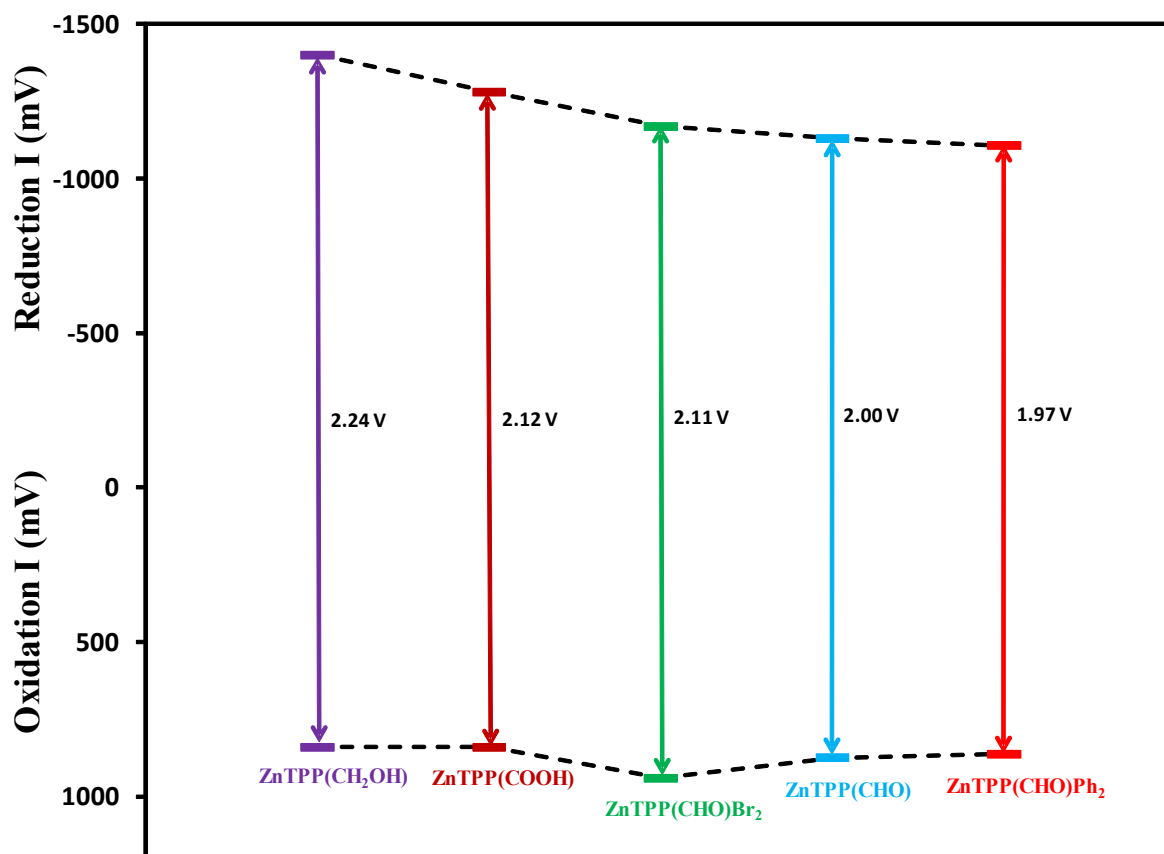


Figure S26. Cyclic voltammograms of (a) MTPP(CHO), (b) MTPP(CHO)Br₂, (c) MTPP(CHO)Ph₂ (d) MTPP(COOH), (e) MTPP(CH₂OH) (where M = 2H, Zn, Cu, Co, Ni) complexes in CH₂Cl₂.

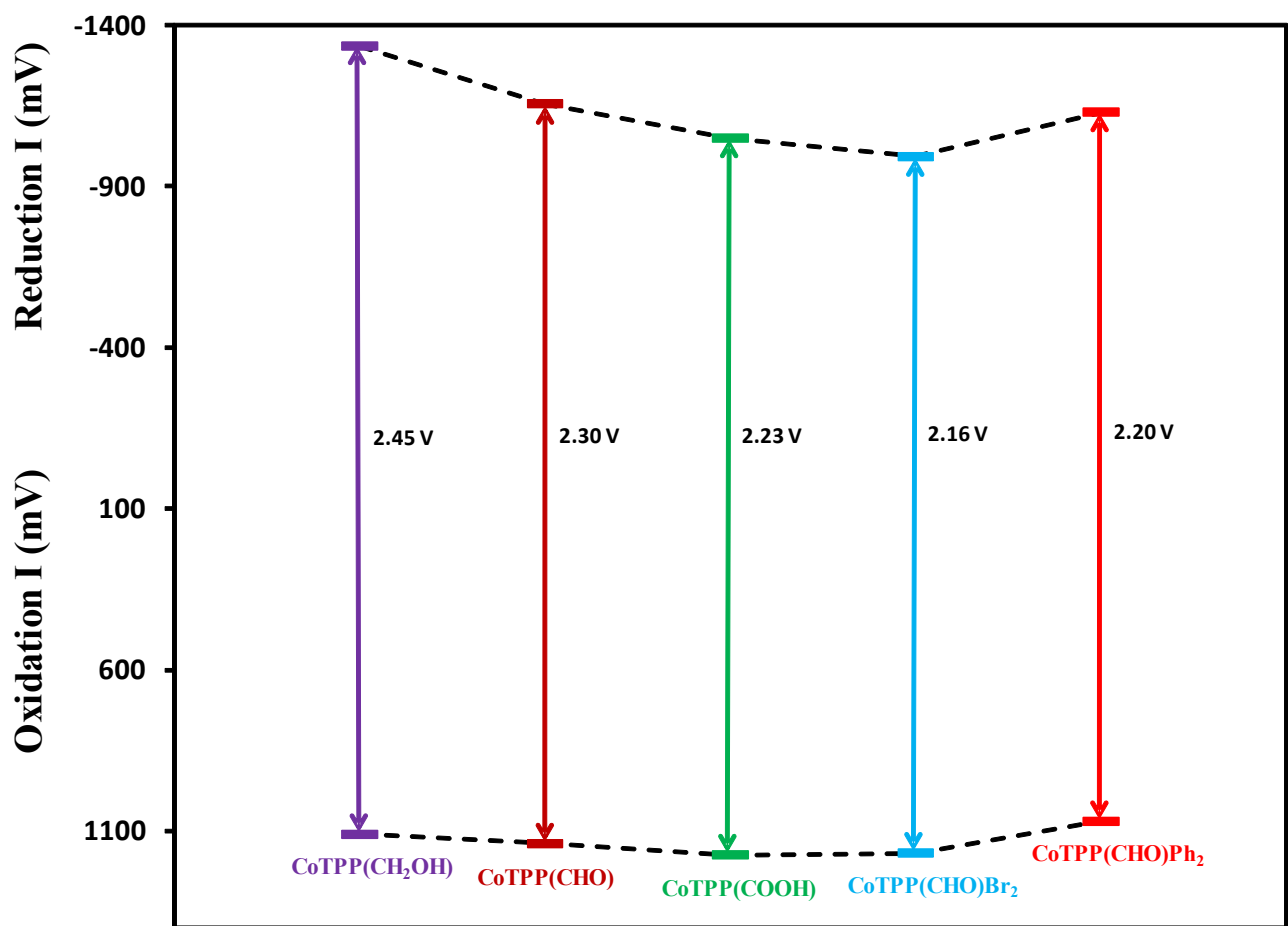
^aContaining 0.1M TBAPF₆ with a scan rate of 0.1 V/s. Pt Working electrode, Ag/AgCl Reference electrode and Pt wire counter electrode were used



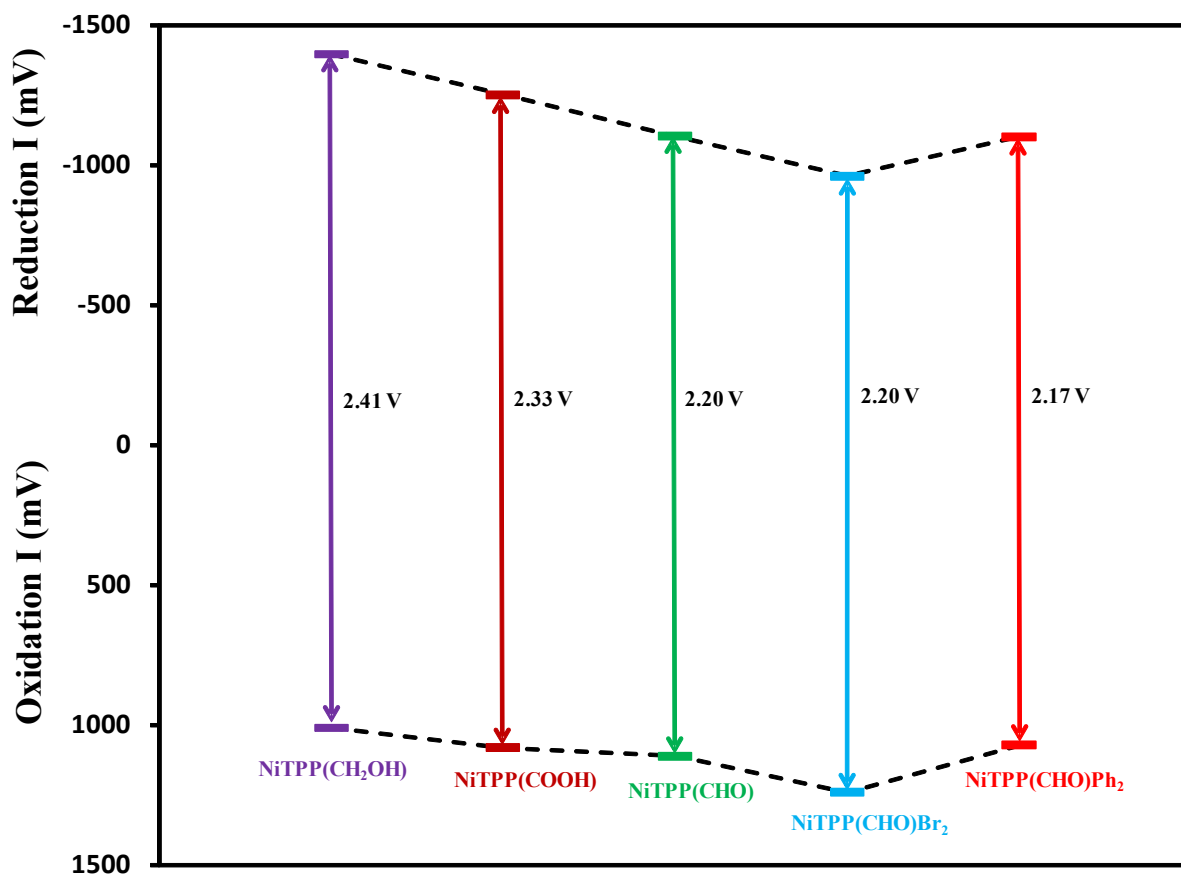
(a) $\text{H}_2\text{TPP}(\text{X})\text{Y}_2^{\text{a}}$



(b) ZnTPP(X)Y₂^a



(c) CoTPP(X)Y₂^a



(d) NiTPP(X)Y₂^a

Figure S27. The HOMO-LUMO variation of various Mixed β -substituted porphyrins: (a) H₂TPP(X)Y₂ (b) ZnTPP(X)Y₂ (c) CoTPP(X)Y₂ (d) NiTPP(X)Y₂ (where X = CHO, COOH, CH₂OH and Y = H, Br, Ph)

^a where X = CHO, COOH, CH₂OH and Y = H, Br, Ph.

Table S4. Modulation of frontier and subfrontier orbitals of CuTPP(X)Y₂ w.r.t CuTPP.

Por.	E _{cg} (eV)	I _{Ox}	I _{Red}	ΔE*(eV)			δϵ _j (eV)	δϵ _i (eV)	δϵ _k (eV)
				ΔE _{cg}	ΔI _{Ox}	ΔI _{Red}			
CuTPP	2.58	0.97	-1.3	-	-	-	-	-	-
1b	2.50	1.06	-1.1	-0.08	0.09	0.20	-0.09	-0.15	-0.20
2b	2.65	0.96	-1.43	0.07	-0.01	-0.13	0.01	0.12	0.13
3b	2.53	1.00	-1.11	-0.05	0.03	0.19	-0.03	-0.26	-0.19
4b	2.47	1.07	-1.1	-0.11	0.10	0.20	-0.10	-0.09	-0.20
5b	2.47	0.93	-1.11	-0.11	-0.03	0.19	0.04	-0.19	-0.19

Table S5. Modulation of frontier and subfrontier orbitals of ZnTPP(X)Y₂ w.r.t ZnTPP.

Por.	E _{cg} (eV)	I _{Ox}	I _{Red}	ΔE*(eV)			δϵ _j (eV)	δϵ _i (eV)	δϵ _k (eV)
				ΔE _{cg}	ΔI _{Ox}	ΔI _{Red}			
ZnTPP	2.54	0.84	-1.36	-	-	-	-	-	-
1a	2.47	0.88	-1.13	-0.07	0.04	0.23	-0.04	-0.30	-0.23
2a	2.55	0.84	-1.40	0.01	0.00	-0.04	0	0.06	0.04
3a	2.51	0.84	-1.28	-0.03	0.00	0.08	0	-0.10	-0.08
4a	2.45	0.94	-1.17	-0.09	0.10	0.19	-0.10	-0.11	-0.19
5a	2.45	0.86	-1.11	-0.09	0.02	0.25	-0.02	-0.30	-0.25

Table S6. Modulation of frontier and subfrontier orbitals of CoTPP(X)Y₂ w.r.t CoTPP.

Por.	E _{cg} (eV)	I _{Ox}	I _{Red}	ΔE*(eV)			δϵ _j (eV)	δϵ _i (eV)	δϵ _k (eV)
				ΔE _{cg}	ΔI _{Ox}	ΔI _{Red}			
CoTPP	2.69	1.06	-1.38	-	-	-	-	-	-
1c	2.54	1.14	-1.16	-0.14	0.08	0.22	-0.08	-0.09	-0.22
2c	2.69	1.11	-1.34	0.00	0.05	0.05	-0.05	-0.05	-0.05
3c	2.65	1.18	-1.05	-0.04	0.17	0.33	-0.12	-0.47	-0.33
4c	2.50	1.17	-0.99	-0.19	0.11	0.39	-0.11	-0.30	-0.39
5c	2.50	1.07	-1.13	-0.19	0.01	0.25	-0.01	-0.12	-0.25

References

1. E. Austin and M. Gouterman, *Bioinorg. Chem.* 1978, **9**, 281.
2. (a) D. M. Jamson, J. C. Croney and P. D. J. Moens, *Methods Enzymol.*, 2003, **360**, 1. (b) M. P. Donzello, G. D. Moria, E. Viola, C. Ercolania and G. Ricciardib, *J. Porphyrins Phthalocyanines*, 2014, **18**, 1042. (c) A. M. Brouwer, *Pure Appl. Chem.*, 2011, **83**, 2213.